SIMPLIFIED REAL-TIME PAH MEASUREMENT TECHNIQUES

by

Timothy L. Pierce

Thesis submitted to the Faculty of the
Virginia Polytechnic Institute and State University
in partial fulfillment of the requirements for the degree of
MASTER OF SCIENCE
in
Mechanical Engineering

APPROVED:

D. R. Jaasma, Chairman

H. H. Robertshaw

T. E. Diller

June, 1982

Blacksburg, Virginia

ACKNOWLEDGMENTS

The author would like to thank Dr. Dennis R. Jaasma for his guidance and many contributions throughout the course of this project. Dr. Thomas E. Diller and Dr. Harry H. Robertshaw are thanked for their advice and for serving on his graduate committee. The author acknowledges the National Institute of Health for a Biomedical Research Support Grant which made this project possible. Special thanks are extended to Jean Dickinson and Roderick Young of the VPI&SU Biochemistry Department for their time and effort spent performing the PAH analysis.

TABLE OF CONTENTS

TABLE OF CONTENTS
(Continued)

LIST OF FIGURES

LIST OF FIGURES
(Continued)

LIST OF TABLES

NOMENCLATURE

$[CO]_s$	mole fraction of CO in the stack
$[CO_2]_s$	mole fraction of CO_2 in the stack
d	Stokes' diameter of a particle
e	collection efficiency
EF_{CO}	CO emission factor, g/kg
EF_{PAH}	PAH emission factor, g/kg
g	local acceleration of gravity, 9.81 m/s^2
K	dimensionless ratio of the range of a particle to the width of the filter paper tape
L	width of the tape, 0.0254 m
$\dot{m}$	instantaneous burning rate, kg/s
m_f	mass fraction of carbon in the wood assuming 10% moisture on a wet basis, 0.46
M_{PAH}	mass of PAH collected each test
MW_C	molecular weight of carbon, 12 g/mol
MW_{CO}	molecular weight of CO, 28 g/mol
$\dot{n}_s$	molar gas flow rate in the stack, mol/s
t	test time, s
v	Stokes' velocity of a particle, m/s
V	stack gas velocity, m/s
ϕ	dimensionless parameter used to correct for conditions in which Stokes' law can not be used to represent the air drag on a particle
λ	range of a particle, m
ρ	density of stack gases, kg/m^3

NOMENCLATURE
(Continued)

σ	particle density, kg/m^3
μ	absolute viscosity of stack gases, Ns/m^2

1. INTRODUCTION

An increase in the cost of home heating in recent years has caused a resurgence in residential wood combustion. This resurgence has increased concern for emissions from wood stoves, especially in areas where such stoves are heavily used. Studies have already been undertaken in Vermont and Alabama to test ambient air conditions in areas of concentrated residential wood combustion (1,2). Polycyclic aromatic hydrocarbon (PAH) emissions are one type of emission from residential combustion and are of great interest because many PAH compounds are known human or animal carcinogens. The problem of PAH emissions from residential wood combustion is emphasized by Peters, et al. (3), who estimate that 38% of national annual polycyclic organic material (POM) emissions result from residential wood combustion. (The terms POM and PAH appear to be used synonymously throughout the literature to name the same basic set of compounds; the term PAH will be used in this thesis.) The problem of PAH emissions is exacerbated by PAH-containing particulate emissions from wood stoves being primarily less than 3 μm in diameter, a respirable size. Thus, the design of wood stoves that emit less PAH is of major importance. Although the magnitude of the problem may not be as great with residential coal combustion (few data exist, but it has been reported that residential coal combustion emits about half the PAH emitted by wood combustion (4)), there is also concern for coal stoves since PAH emissions are still high (by at least an order of magnitude) compared to oil and gas heating units.

Efforts to reduce PAH emissions by improved stove designs have been hampered by the cumbersome nature of presently-used PAH measurement techniques. A typical method of determining PAH emissions is to collect samples with filters and organic traps, extract the PAH compounds, and then analyze the solvent extract for the PAH compounds using some type of chromatography and/or mass spectrometry. This method of determining PAH emissions is slow, expensive, and complex. A delay of two days can be expected between the time a sample is collected and the PAH compounds are quantified. An expensive laboratory set-up is needed to collect samples and analyze them, and trained personnel are required to operate the equipment. An estimated cost of $1500 per sample might be expected just for an out-of-house analysis of a sample. Because of these drawbacks a simplified real-time PAH measurement technique would be of great value.

The purpose of this study is to investigate simplified real-time PAH measurement techniques for residential wood and coal combustion. A real-time system has several advantages over present methods of testing stoves. It allows the effects of controllable variables (such as air control settings) on PAH emissions to be quickly determined, within the limitations imposed by the fact that repeated burn cycles of the stove may give different PAH emissions (and possibly different responses to the variable) due to differences in fuel bed conditions. A real-time measurement device would also quantify PAH emissions throughout the burn cycle, thereby determining what parts of the burn cycle should be concentrated on most when considering stove modifications. Simple and

inexpensive real-time measurement techniques have the further advantage that stove manufacturers (generally small and technologically unsophisticated companies) could use such methods if desired or necessary.

In this report two real-time PAH measurement techniques are investigated. The first, called the "moving tape sampler" (MTS), is a device that attempts to collect and measure PAH compounds from the stack of a stove. The second method is the use of a proxy compound which correlates with PAH emissions. Neither of these methods is expected to have a high degree of accuracy, but if they are inexpensive enough their usefulness in determining relative amounts of PAH emissions may outweigh this limitation.

The detection method used by the MTS is sensitized fluorescence. Smith and Levins (5) showed that a sample of PAH mixed with sensitizer fluid and spotted onto filter paper fluoresces in visible wavelengths when illuminated with a 254 nm ultraviolet light source. The intensity of the fluorescence was found to be an indication of the amount of PAH in the sample. This method has been shown in some cases to give reasonable order of magnitude estimates of PAH emissions from both fireplaces and airtight stoves (6). The MTS is an automated version of this method, using filter paper tape in a train that can continuously collect and analyze samples from the stack of a residential wood or coal stove.

In order to validate the MTS as an effective measurement technique, its results must be compared to a "conventional" PAH measurement technique. For this study, this is done using glass fiber filters

located above the stack to collect, for a short period of time, all the smoke from the stove's exhaust. (The term "smoke" is herein defined as combustion-generated matter consisting mostly of condensed hydrocarbons.) The catch from the filters is analyzed by gas chromatography to determine the amount of PAH collected. This "total collection" technique was first used by Butcher and Sorenson (7), who did not perform PAH analysis on the samples they collected. The results of the two methods are compared to determine if any relationships exist between the MTS results and "conventional" results.

The second method is the use of CO and NO_x as proxy compounds to infer PAH emissions. The idea of using a proxy to infer PAH concentrations is not new, as it has been tried for workplace monitoring of PAH (8). Published emission factors for CO, NO_x, and PAH are plotted in an effort to show any relationships between the proxy compounds (CO and NO_x) and PAH emissions. The CO emissions measured while testing the MTS are also plotted against the PAH emissions determined from the filter catches. Unfortunately, NO_x emissions were not measured during this investigation because of a malfunctioning NO_x analyzer.

2. LITERATURE REVIEW

2.1 PAH Emissions

2.1.1 Emissions Data and Measurement Techniques

Before the recent renewed interest in residential wood and coal combustion systems, studies measuring PAH emissions from these systems were limited to a few reports considering only coal. Since 1980, several major studies concerning PAH emissions from residential wood combustion have been performed, but even with this recent research the emission factors (ratios of the mass of pollutant emitted per mass of fuel burned) are still not well known. The following summarizes the available information on PAH emissions from residential wood and coal combustion and points out the problems, inconsistencies, and uncertainties associated with these emissions and the measurement techniques used to obtain them.

One of the earliest reports on PAH emissions from combustion systems is by Hangebrauck, et al. (9), who investigated heat generation processes which burn conventional fuels. Coal, oil, and gas were burned in equipment ranging in size from heavy industrial power plant boilers to residential heaters. Samples were collected from the stack gases using a train designed to condense organic compounds. A 99% collection efficiency for PAH (the percentage of PAH recovered when probing known concentrations) was reported. The method used to obtain this figure was not discussed and would be of interest since a recent study (10) reported difficulties in obtaining efficiencies even close to 99%. Ultraviolet-visible spectrophotometry (the detection of compounds from

their own associated fluorescence wavelengths) was used to detect PAH compounds in the samples collected. Emission factors expressed as grams of pollutant emitted per kilogram of fuel burned were less than 0.001 g/kg for all the systems except the two residential heaters burning coal, which yielded emission factors of 0.003 and 0.2 g/kg. Important conclusions drawn from the results of this study were that coal-fired units would be expected to emit more PAH (per mass of fuel burned) than oil and gas fired combustors and that the residential combustion units had higher emission factors than the larger industrial units. Sampling from the stacks was reported to be isokinetic, which would require accurate stack gas velocity measurements. Although the method of determining stack velocities was not discussed, it is expected that problems were encountered in measuring the small velocities from the residential heaters. These velocities (on the order of 1 m/s) yield pitot-tube pressure differentials of ca. 25 Pa (difficult to measure accurately) and have velocity profiles about which little is known. This problem of inaccurate stack gas velocity measurements is a likely source of error in the coal stove PAH emissions reported by Hangebrauck. The other studies discussed in this section also did not use accurate velocity measurement techniques, and this weakness is a source of error in their reported PAH emission factors. The magnitude of this error is uncertain.

Few studies on PAH emissions were performed in the late 1960's and early 1970's. In 1967 Diehl, et al. (11) discussed PAH emissions from coal-fired installations and concluded that PAH concentrations in the

stack gases of commercial coal combustors can be highly variable and are not easily related to changes in operating parameters. They did not investigate residential combustors. In 1972 the National Academy of Sciences (12) published a report that summarized the limited data then available on PAH emissions from stationary sources. The report points out a lack of data on emissions from wood combustion and calls for work in this area.

Giammer, et al. (13) measured and reported PAH emission factors for residential and small commercial stoker coal-fired boilers. They sampled for PAH with a modified EPA Method 5 sampling train. The modification to the Method 5 train was the addition of an organic trap to collect gas-phase PAH. The method of identifying PAH compounds in the collected samples was not discussed. The reported emission factors ranged from $3. \times 10^{-4}$ to 0.2 g/kg, and the authors suggested that coals with a high volatile content and free swelling index (a measure of the caking property of a coal) tend to yield high PAH emissions.

DeAngelis and Reznick (14) tested a residential coal-fired furnace and boiler and reported PAH emission factors obtained using a modified Method 5 sampling train. The PAH collected by the train was extracted with several solvents and analyzed by means of gas chromatography and mass spectrometry (gc/ms). A slightly higher range of emission factors (0.02 to 0.3 g/kg) was reported. This study also showed that higher coal volatile contents gave higher PAH emissions and suggested that increasing excess air may reduce PAH emissions.

The first measurements of PAH emissions from wood stoves were performed by DeAngelis, et al. (6). Baffled and non-baffled wood stoves and fireplaces were tested using the modified Method 5 train to collect stack samples. Several solvents were used in the extraction process and a gc/ms work-up was used to quantify PAH compounds. They used the spot test of Smith and Levins (5) in an attempt to screen for PAH compounds before the gc/ms analysis. For the spot test, a simple sampling train with three impingers containing methylene chloride was used to collect flue gases during part of the time the modified Method 5 train sampled. The collected samples were subjected to the spot test, using known amounts of Benzo(a)pyrene (BaP) to produce fluorescence intensities for comparison with the fluorescence of the sample mixture. The mass of PAH in the sample was defined to be the mass of BaP which gave nearly equal fluorescence; it is unclear whether this is a reasonable assumption. These field tests predicted the correct range of PAH for two fireplace tests, but differed by factors of 2 to 15 for the wood stoves. There are problems in this method of comparison since the spot test was conducted on samples collected from a separate and different train which only sampled part of the time the Method 5 train sampled. Thus, results from the Method 5 train are averaged over a longer time period. Better (or worse) results for the screening may have been obtained if the spot test had been conducted on samples taken from the Method 5 train. The wood stoves gave high PAH emissions, ranging from 0.19 to 0.37 g/kg for four tests. The fireplace yielded lower PAH emissions, with an emission factor of 0.03 g/kg for two tests burning different types of wood. High

burning rates (6.0 to 8.4 kg/hr, equivalent to heat delivery rates of ca. 16 kW) were used for the stoves in this study and probably are not representative of burning rates typically used in residential combustion.

Much of the available data on PAH emissions is available in the proceedings of the 1981 International Conference on Residential Solid Fuels. Cooke, et al. (15) tested commercially available stoves employing updraft, downdraft, sidedraft, and turbulent modes of burning. They sampled stack gases with the modified Method 5 technique and analyzed the samples with a capillary gc/ms procedure. This gc/ms technique was an improvement over past methods, since the use of the capillary column allowed more compounds to be separated on the gc curve. This reduces the chance that a compound's concentration will be overestimated because two or three compounds elute almost simultaneously, forming one peak instead of two or three. Emission factors ranged from 0.01 to 0.05 g/kg, with the turbulent burner (a specially designed, forced-air burner that promotes turbulence) exhibiting the lowest emission factor and the downdraft mode the highest. A comparison with the results of DeAngelis (6) for similar conditions (burning seasoned oak at a high burning rate in the updraft mode) shows emission factors of 0.018 g/kg for this study versus 0.19 g/kg for DeAngelis, an order of magnitude difference. It is not clear whether this difference is due to different PAH emission levels or differences in the measurement techniques used.

Rudling, et al. (16) investigated burning of both logs and wood chips in a heating furnace and logs in an airtight stove. The sampling train used to collect stack gases included a borosilicate fiber filter thimble, a condenser which cooled the gases to 5-10°C, and finally an organic trap for collecting gas-phase PAH. A large range of PAH emission factors (0.005 to 0.14 g/kg) was found for the stove. Their highest emission factors seem to correlate with high fuel moisture content (>40% -- basis not given) and a reduce air flow.

Hubble, et al. (17) also used a modified Method 5 train and gc/ms procedure to determine PAH emissions from a stove operating at two different burning rates. The two emission factors, 0.004 and 0.008 g/kg, were obtained at burning rates of 0.82 kg/hr and 7.7 kg/hr respectively. The value of 0.008 g/kg was obtained at conditions similar to those used in the earlier comparison between Cooke and DeAngelis, and is about half the value found by Cooke.

The effect of high altitude (low pressure, 626 mm Hg) on wood combustion was tested in the work of Peters, et al. (18). The testing conditions used by DeAngelis (6) (burning seasoned oak in a non-baffled stove) were duplicated so that the results of this study could be compared to low altitude (barometric pressure of 745 mm Hg) results. A PAH emission factor of 0.05 g/kg was found by averaging two runs. This result is about one-fourth the value determined in the low altitude study. The authors suggested that lower combustion zone temperatures due to the cool (9°C) ambient air source could have retarded PAH forming mechanisms and thus caused the lower emission factor. This report could

have been used as an indicator of test repeatability, but the authors neglected this potential and reported only the average value for the two runs. No data on the repeatability of presently-used PAH measurement techniques have appeared in the literature to date.

Cooke and Allen (19) have suggested a standardized protocol for sampling and analyzing organic emissions (which include PAH emissions) from wood stoves. A modified Method 5 sampling train is proposed for collecting stack gases and a detailed procedure for analyzing the samples is given. For accurate determination of PAH emission factors, this method (and the others previously discussed) depends on a knowledge of what percentage of the effluent is quantitatively analyzed. For large-scale combustion systems, this percentage is determined by sampling isokinetically from the stack and using the probe-to-stack area ratio to represent the percentage of flow collected. Cooke and Allen's protocol does not have an accurate method of determining stack gas velocities. Since this is necessary for isokinetic sampling, the accuracy of the protocol is limited by the degree to which isokinetic sampling occurs.

Although the modified Method 5 sampling train is presently considered the best method of collecting PAH compounds, Sonnichen, et al. (10) have shown that recovery problems exist with a sampling train similar to this type. They injected known amounts of deuterated PAH into a sampling system that was concurrently collecting samples from a coal-fired power plant. The recovery of these tracer compounds ranged from two orders of magnitude less than the injected amount to several

times more. No similar experiments have been performed for wood stove PAH measurements, and there is reason to believe that if such experiments were done the results would be no better. There is great difficulty in quantifying species from streams which contain combustion-generated particulate.

2.1.2 PAH Proxies

Literature on the use of proxies for PAH concentrations is scarce. The following discusses the available papers and shows that the use of proxies has been considered for some time.

The use of CO as an indication of PAH concentrations in emissions from oil, gas, and coal combustion systems was apparently first considered by Hangebrauck, et al. (9), who suggested that high CO emissions could be used as an indication of high PAH emissions. However, this idea could not be supported from their data since the relationship between PAH and CO was too inconsistent.

The idea of proxy compounds for PAH monitoring in workplaces is discussed by Gammage and Bjorseth (8), who considered CO as a possible proxy for PAH concentrations in coal gasification plants. The use of BaP (one of the more carcinogenic compounds and sometimes thought to be a good proxy for the potential danger from PAH) as a proxy for PAH compounds is heavily criticized and the use of BaP for workplace monitoring is not recommended.

Pierce and Jaasma (20) have pointed out the inadequacy of BaP as a proxy compound for wood stove PAH emissions. Using the data of Cooke,

et al. (15) they showed that PAH/BaP ratios varied from 13 to 1300, a range which eliminates BaP as a useful proxy.

The use of CO and NO_x as possible proxy compounds for PAH emissions from wood stoves has been suggested by Jaasma and Metcalfe (21). They plotted DeAngelis' data (6), which suggest that PAH emissions from wood combustion will be high when CO emissions are high and NO_x emissions are low. The authors also suggested unburned hydrocarbons or total condensable organics and particulates (smoke) as other possible proxies of PAH emissions.

Wainwright, et al. (22) concluded that visible smoke conditions seemed to estimate PAH emissions in tests conducted on industrial wood-fired boilers but did not offer conclusive evidence. The PAH emission factors for this type of equipment ranged from $2. \times 10^{-5}$ to 0.003 g/kg.

2.1.3 Summary

For wood stoves, the available data on PAH emissions are limited to long-term stack sampling tests (compared to the 60-105 s sampling intervals used in this study) and show a range of emission factors of 0.004 to 0.37 g/kg, almost two orders of magnitude. Even tests conducted under similar conditions show a range of 0.008 to 0.19 g/kg. This indicates that either inconsistencies exist between the methods used in various studies or the run-to-run variation in emissions is very high. The inconsistencies probably include differences in equipment, test conditions, sample trains, sample analysis, and stack gas velocity

measurement techniques. Because of all these possible variations and little knowledge of how each affects measured PAH emissions, a standard method of measuring PAH emissions from wood and coal stoves is needed and should be validated inasmuch as possible. Cooke and Allen's protocol with the addition of an accurate stack gas velocity measurement technique and a group of compounds defining PAH emissions is a logical starting point. The modified Method 5 sampling train should be tested for collection efficiency with experiments spiking the sampling probe with known amounts of deuterated PAH. The group of compounds for PAH identification could be based on carcinogenicity or stack gas concentrations, while a dilution tunnel could be employed for accurate stack gas velocity measurements (23).

The use of proxies for PAH emissions from combustion systems is only briefly discussed in the literature. Carbon monoxide and NO_x have been suggested as possible proxy compounds for PAH emissions from wood stoves, but experimental studies testing these compounds as proxies have not been performed.

2.2 Particulate Deposition

The collection of particles from the wood stove effluent is an important factor in the successful operation of the MTS. The ability to theoretically predict the particle depostion rate to the tape would be a valuable tool in evaluating the MTS. A review of the literature on particle deposition is given to assess the particle deposition phenomena which occur with the MTS.

One of the first works on particle deposition is by Langmuir, et al. (24) and looks at the trajectories of water droplets (in fog) about a cylinder, sphere, and ribbon. The study only considers particles deposited by inertial impaction, i.e. those particles that do not follow the flow around the obstruction in the gas stream and instead are carried into the obstruction by their inertia. By solving the equations of motion for the particles, graphs for the collection efficiency were developed in terms of the dimensionless parameters K and ϕ. The collection efficiency (for the MTS) is defined as the ratio of the particles impacted on the tape to the number that would have impacted if the particles traveled in straight paths to the tape. The parameter K is a ratio of the range of a particle to the radius of the collection cylinder or sphere (width in the case of a ribbon). The range is the distance a particle (given an initial velocity) will travel in a fluid before being brought to rest by the resistance of the fluid, assuming Stokes' law holds. The parameter ϕ is used for conditions where Stokes' law can not be used to represent the air drag on the particles. The graphs show that values of K (for ϕ = 0 to 10^4) greater than 0.1 are needed for inertial impaction to occur. Although this report does not directly deal with the impaction of smoke particles in a gas stream, it is the basis for further studies in inertial impaction.

Johnstone and Roberts (25) looked at the deposition of aerosol particles from moving gas streams, considering both impaction and diffusion. The paper looks at the theory of impaction presented by W. Sell in 1931. These results are a simpler form of the curves presented

by Langmuir and are restricted to small particles (those in which Stokes' law holds). For particle diameters less than 0.5 μm, it is thought that the rate of deposition will become greater by diffusion than by impaction. The efficiency of deposition by diffusion is discussed, but only for collection on spheres. This efficiency is found to be dependent on the diffusivity of dust particles and the effective film thickness due to the gas flowing around the sphere.

Jordan (26) investigated the ability of particles to adhere to a surface upon contact by looking at the forces acting on the particle as it comes in contact with the surface. He defined a critical velocity as the velocity that a particle must be less than (relative to the surface) if it is to adhere to the contacting surface. A critical velocity of 0.3 m/s is estimated for a 1 μm diameter, spherical, quartz particle contacting a clean, dry surface. The ability of particles to continue to adhere to a surface after initial deposition is also discussed. High velocity (>50 m/s) air streams flowing over a dry sample plate removed no more than 20% of the original ($\leq$ 6 μm) particles (glass and quartz) on the plate. Jordan's work suggests that the slow velocities in a flue (around 1 m/s) will be ideal for the adhesion of particles contacting an obstacle in the gas stream.

A paper by Unger and Putnam (27) discusses the different aspects of particle deposition in boilers and turbines. They conclude that the physical factors influencing particle deposition include the intensity of particle movements relative to the stream, flow velocities, level of stream turbulence, temperature and pressure of the gas carrying the

particles, and concentration of the particles. All these conditions influence the speed and direction of the particles, which in turn determine whether the particles will deposit on a surface. The basic mechanisms of deposition are grouped into four categories, molecular diffusion, random walk, turbulent diffusion, and inertial impaction. Molecular diffusion is the main factor of deposition for particles less than 0.1 μm. In this case the authors consider particles to "slip" between molecules. Random walk is the diffusion of particles due to Brownian motion, i.e. the movement resulting from bombardment of gas molecules. Turbulent diffusion is a result of particles being moved by eddies and whirls in the gas stream, while inertial impaction becomes important as the particles become too large to follow the flow lines of the gas. Unfortunately, this paper is limited to a discussion of the four mechanisms, and methods of calculating collection efficiencies are not presented.

Golovin and Putnam (28) reviewed inertial impaction on single elements such as cylinders, spheres, ribbons, and airfoils. The basic equations and graphs developed by Langmuir are presented and it is pointed out that the use of Stokes' law in Langmuir's derivation postulates that the particles are spherical and experience the fluid as a continuum. To correct for this assumption, a correction term known as the Cunningham or Millikan correction can be applied. Fortunately, at normal pressures and temperatures and particles sizes as low as 1 micron the correction term is nearly unity and can be neglected. The impaction efficiencies for ribbons normal to a flow are presented in graphical

form and a comparison of all the elements shows that the ribbon yields the highest impaction efficiency.

Noll and Pilat (29) compared theoretical and experimental results for inertial impaction upon rectangular bodies. Three potentials flow described as ribbon flow (flow around a ribbon normal to the flow), half body flow (flow around a rectangular half body), and hyberbolic flow (hyberbolic flow lines that would result in a corner with infinite sides) are considered. Good agreement is found between the theoretical and experimental results as long as the experimental flows were considered as potential flows.

Hawskley, et al. (30) address the theoretical aspects of sampling particles in flue gases. Collection efficiencies by impaction are discussed and the graphs by Langmuir are presented. Particle sizes in wood smoke are predominantly submicron (31), and so only the curves assuming Stokes' law holds ($\phi = 0$) are applicable. An equation for collection efficiency in terms of a parameter similar to the K used by Langmuir is also presented which is a result of linearizing Langmuir's equations of motion. The two techniques are found to be in good agreement, and thus the equation can be used for quick estimates of the collection efficiency by impaction. The single curve presented by Hawskley is used to estimate the collection efficiency of the MTS in Section 5.1.

3. APPARATUS AND PROCEDURES

3.1 Experimental Apparatus

3.1.1 The Moving Tape Sampler

A schematic of the MTS is shown in Fig. 1. Filter paper tape (Schleicher and Schuell #410) is drawn at 1 cm/s from a roll and through the MTS by a dc motor. The tape enters the exhaust stack perpendicular to the flow so that the flat surface of the tape faces the rising exhaust. The tape passes through the stack and collects particulate matter from the gas stream. In the middle of the stack, the tape runs under the open end of a 6 mm diameter stainless steel tube. The other end of the tube is attached to a suction pump which draws gases through the tape. The tape exits the stack and is then twisted approximately 135° by three guides. The guides are arranged so that the side of the tape containing the sample (the downside of the tape as it exits the stack) never comes in contact with the guides. With the sample-containing side now facing upward at a 45° angle, a pressurized (200 kPa) cylinder forces sensitizer fluid onto the tape. This fluid consists of napthalene in methylene chloride (60 g/litre). A schematic of the cylinder is shown in Fig. 2. A cock value is used to turn the flow on and off, while a microvalve is used to set the flow rate. The microvalve was generally set at one turn open.

The sensitizer-wetted filter paper passes through a dryer to evaporate the methylene chloride. The dryer consists of a chamber with warm air blown in from a heater and exiting through an opening in the side opposite the inlet. The dried tape enters the detection module,

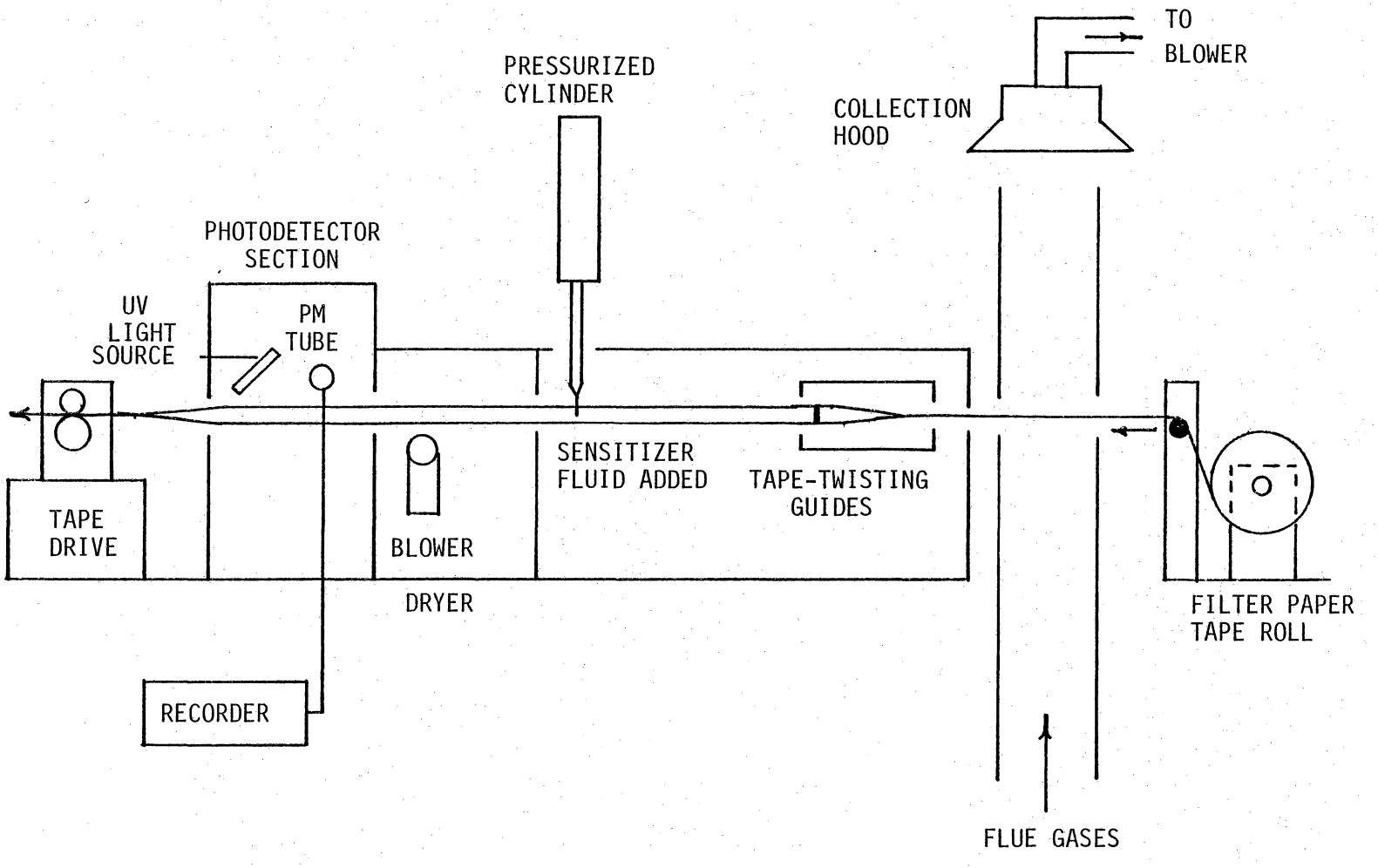

Figure 1. MTS Schematic.

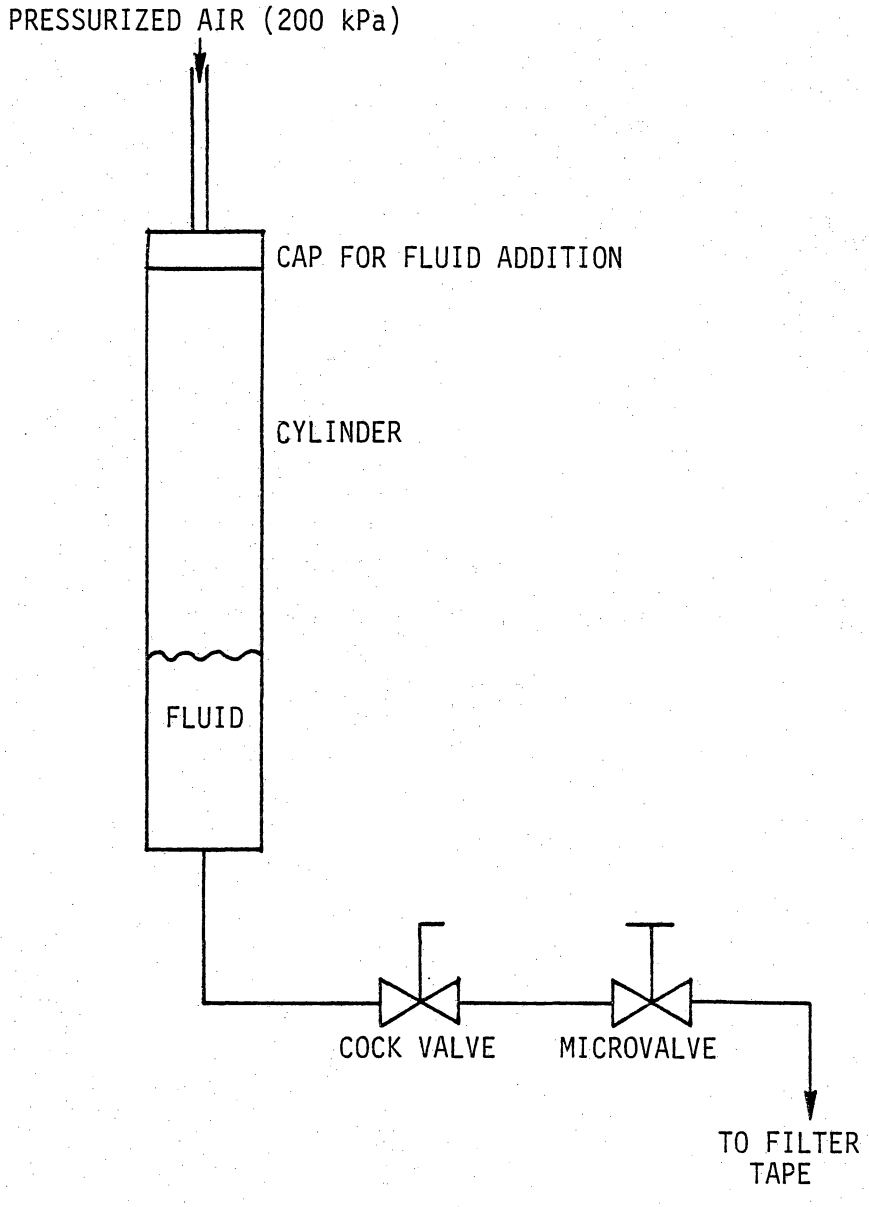

Figure 2. Pressurized Cylinder Schematic.

which is a box containing an Ultra-Violet Products, Inc., UVS 11, 254 nm ultraviolet light source and an RCA 931-B photomultiplier tube. Figure 3 shows the relationship between the light, tube, and tape. The tube is connected to an RCA PF 1042 power supply which supplies the high voltage needed to operate the tube. The tube and power supply are enclosed in a 5 x 5 x 22 cm box. A slot in the box, facing the tape, allows light to enter the cathode of the tube. A Schott GG 400 sharp cut off filter rests in front of this slot and is used to try and reduce the signal to noise ratio. Figure 4 shows the characteristics of the GG 400 filter, which cuts out wavelengths less than approximately 400 nm. Tests with a scanning spectrometer showed that light emitted from the tape containing just sensitizer fluid is of a shorter wavelength than that emitted by the sample-sensitizer fluid combination. The filter is used to cut out the light from the sensitizer alone while allowing light from the sensitizer and sample to pass. The tape finally leaves the detection module and is pulled through the tape drive mechanism. The tape drive consists of two parallel cylinders running together. The top cylinder is connected to a dc motor with two gears to reduce the rotational speed from the motor. The tape passing through the drive is discarded.

The current output of the tube indicates the amount of visible fluorescence from the tape. This output is converted into a voltage with a 40 kilohm resistor and measured with both a voltmeter and stripchart recorder.

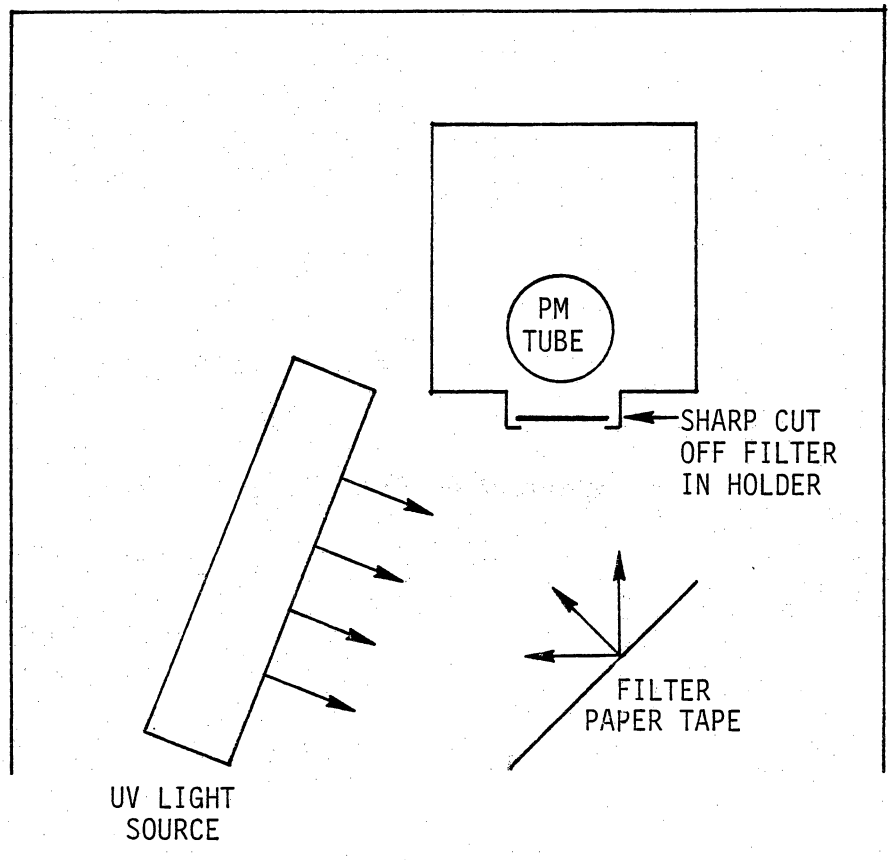

Figure 3. Photodetector Schematic.

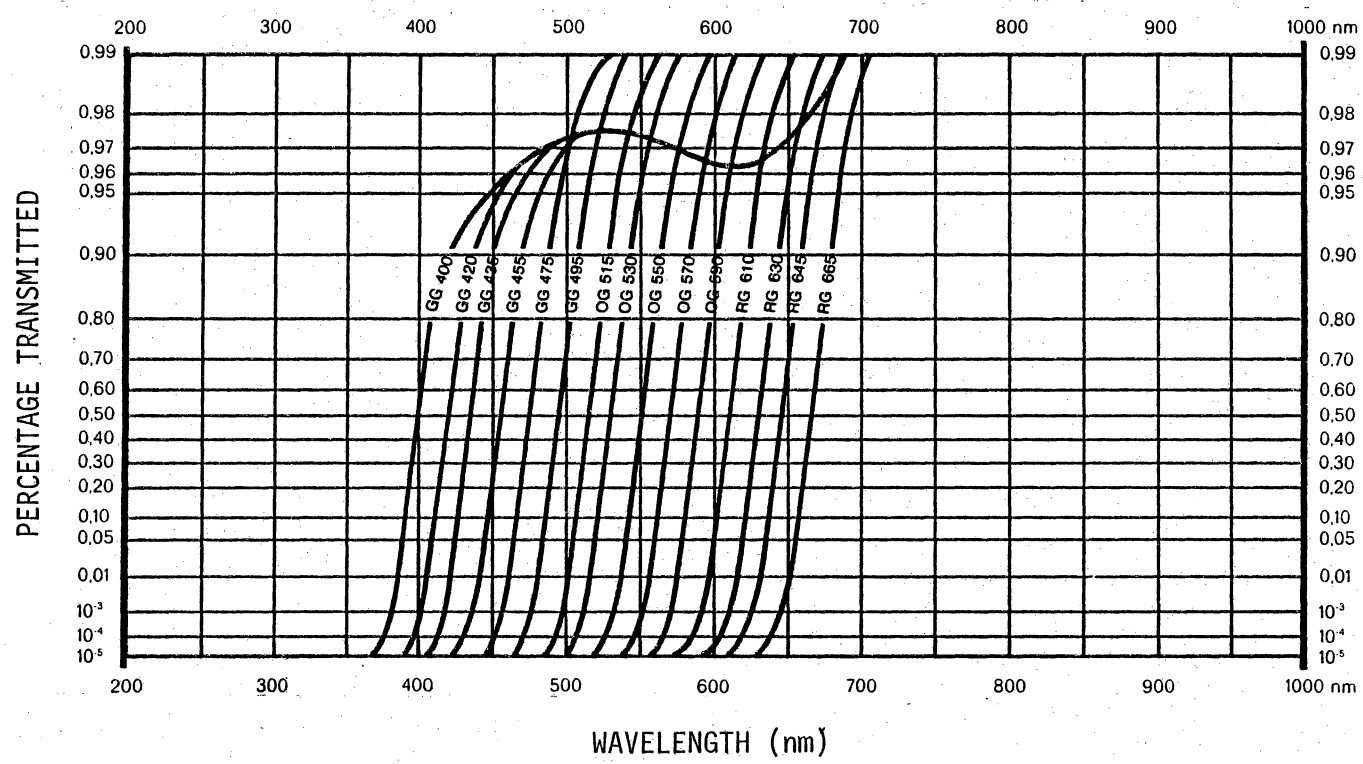

Figure 4. Transmission Curve for the GG 400 Color Filter Glass.

3.1.2 General Set-up

The set-up used for testing the MTS is shown in Fig. 5. A Shenandoah Manufacturing Co., Inc. stove (model R-76LC) was used and is shown schematically in Fig. 6. The stove is a radiant heater and has both primary and secondary air inlets as shown.

The stove was situated beneath a 7 m high steel frame that contained 3 platforms at heights of 2 m, 4 m, and 6 m. A 15 cm diameter, 24 gage, galvanized steel flue pipe was connected to the stove and extended 6.5 m up through the frame and platforms. This length of pipe allowed the stove to operate under natural draft conditions. The MTS was mounted on the top platform near the end of the stack.

A collection hood was supported just above the outlet of the flue pipe. A dilution tunnel attached to the top of the hood was used to draw in the exhaust gases and some ambient air and to determine stack gas velocities (23). A high pressure blower exhausted the mixture through a vent to the outside. The collection hood was designed to allow for the insertion of 20 x 25 cm glass fiber filters (Gelman no. 61635). The filters were used to collect the smoke from the flue gases. The hood was made so that the filters could be readily changed and thus could be inserted for brief periods of time. The catches from the filters were used for "conventional" PAH analyses, which were compared to the MTS signal.

Two type K thermocouples (chromel-alumel) were placed in the stack, one 2 m above the stove and one at the top near the MTS. This second thermocouple was used to measure the temperature of the exhaust gases

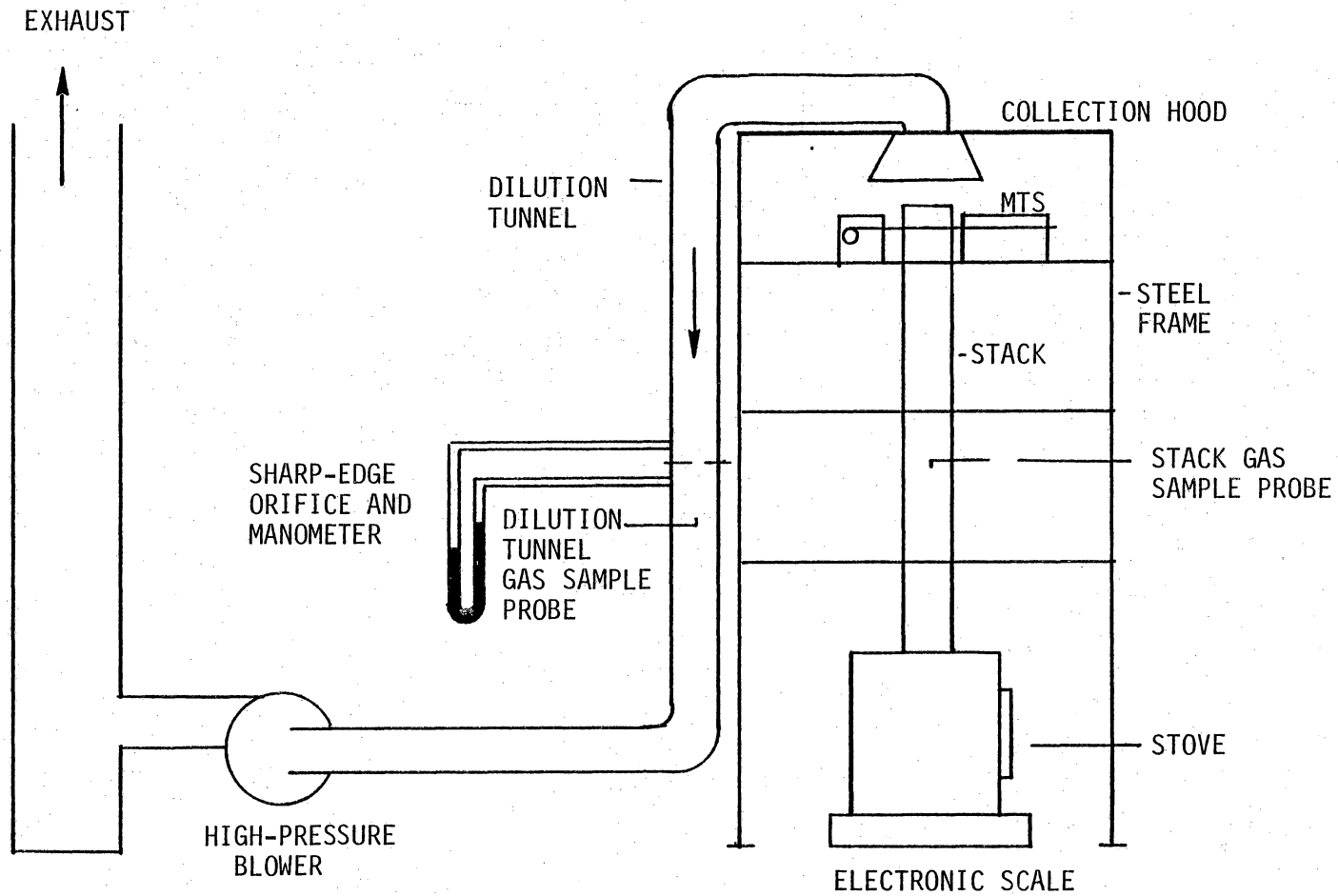

Figure 5. Stove and Flue Gas Handling System Used to Test the MTS.

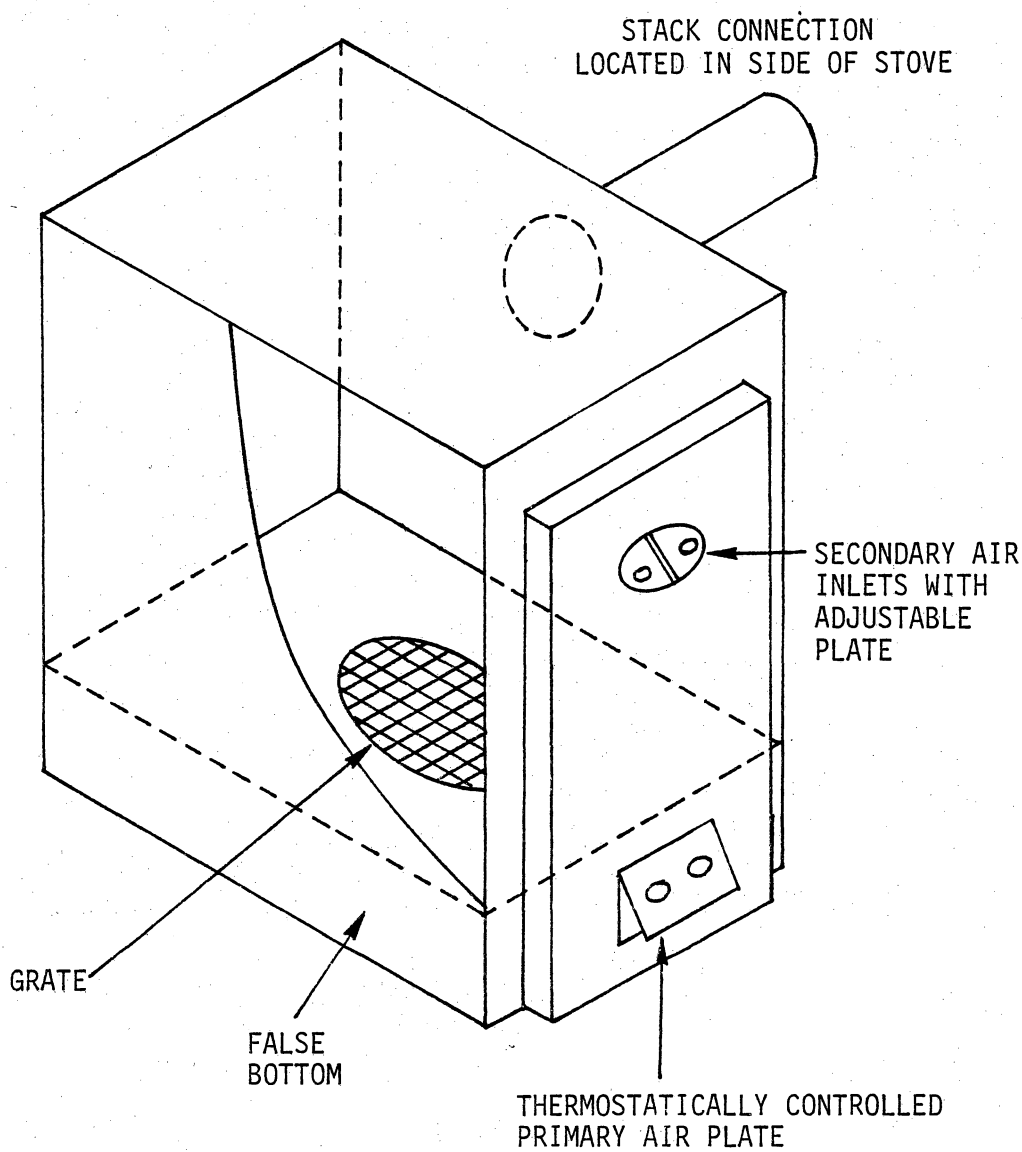

Figure 6. Schematic of the Shenandoah (R-76LC) Stove.

flowing past the filter paper tape. A thermcouple was also placed in the hood to monitor the temperature of the gases downstream of the filter.

The molar flow rate in the dilution tunnel was measured with a sharp-edge orifice plate. A manometer was used to measure the pressure drop across the orifice and another type K thermocouple measured the temperature of the gases passing through the orifice.

An electronic scale supported the stove and was used to determine the mass-time history of each charge placed in the stove.

Figure 7 shows the gas sampling train used to monitor the concentrations of CO and CO_2 in the stack and dilution tunnel. A switching valve was used to connect the sampling train to either the stack or dilution tunnel. The gases removed from either the stack or dilution tunnel were passed through a 0°C condenser to remove moisture and a filter to remove particulates. A sample pump delivered the gases to a CO/CO_2 analyzer (Infrared Industries IR 702) which provided a nearly real-time indication of CO and CO_2 concentrations. The gases leaving the analyzer were allowed to flow back into the dilution tunnel.

3.2 Experimental Procedure

Prior to each run the ash in the stove was removed. The CO/CO_2 analyzer was spanned and calibrated according to the instrument manual instructions. The MTS was prepared for testing by warming up the photomulitplier tube, filling the pressurized cylinder with sensitizer fluid, and adjusting the air pressure to 200 kPa. The motor drive was

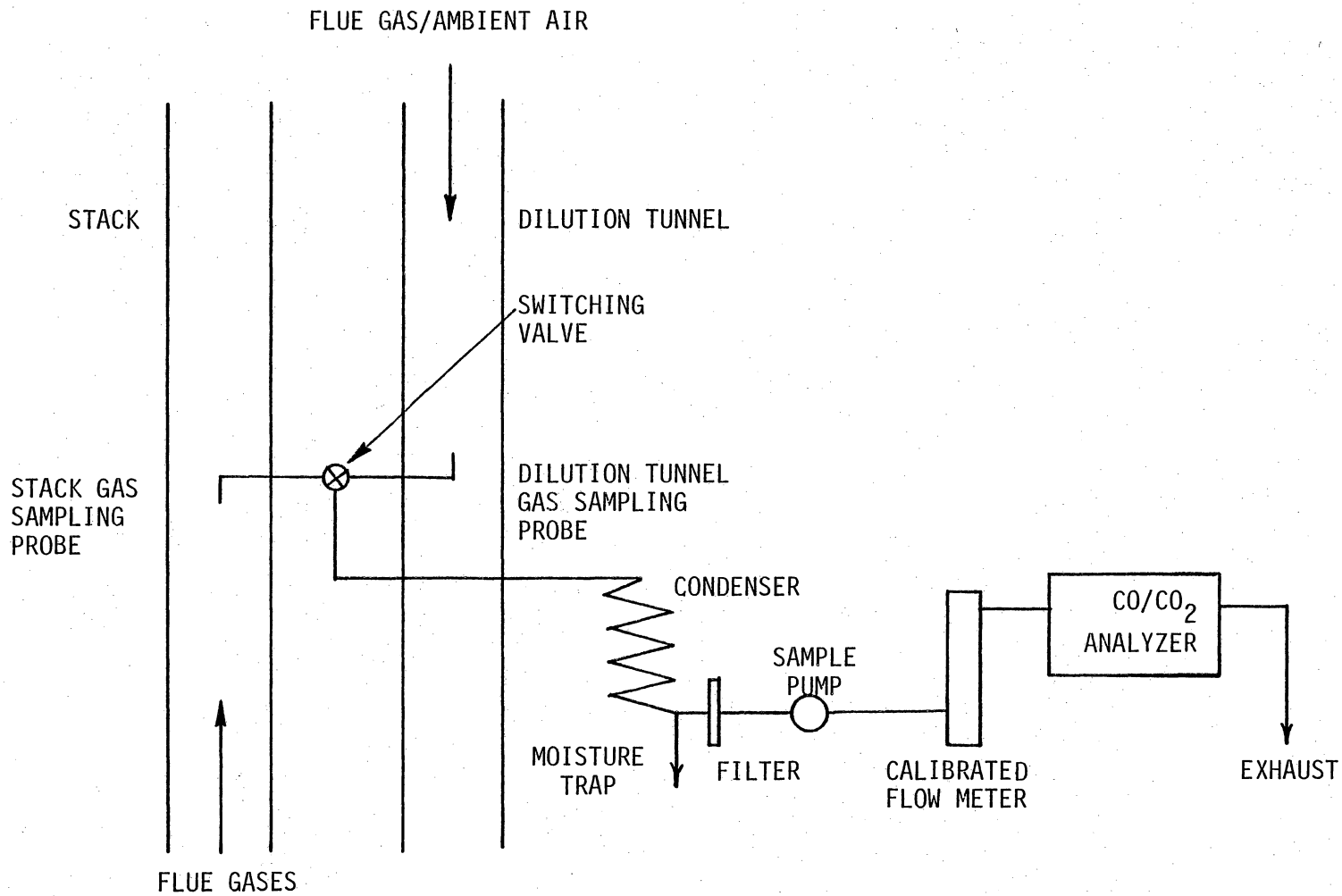

Figure 7. Sampling Train Used to Analyze Stack and Dilution Tunnel Gases for CO and CO_2 Concentrations.

started and the valves from the cylinder were opened, allowing fluid to flow onto the filter tape. The output of the photomultiplier tube was observed on the chart recorder and taken as a "zero" point or an indication of zero PAH. The only fluorescence seen by the tube at this point was due to the sensitizer fluid. Finally, a protective channel was placed in the stack around the filter tape to shield the tape from the exhaust gases. The channel could be used to redetermine the zero point once the stove was ignited and also was used to protect the filter tape from sparks when the tape was not moving.

When the MTS and sampling train were ready for testing, the blower was turned on and a fire was started with kindling. After a few minutes, a charge of split, dry oak (3 or 4 pieces with a total mass of 5-10 kg) was placed on the stove. Once the charge had become well ignited, testing of the MTS began by starting the motor drive, sensitizer fluid flow, and suction pump. The protective channel was removed from the stack, allowing the filter tape to begin sampling. A glass filter was inserted in the collection hood and the chart recorder was started. A stop watch was used to determine the time the filter was in place. This time, defined as the test time, varied (30-105 s) depending on how rapidly the glass fiber filter in the hood became loaded. Under heavy smoke conditions the filter would become loaded quickly and would then not allow all the exhaust gases to pass through it. This would cause the filter to not collect all the PAH from the stack and would underestimate the "conventional" PAH results. After several tests, the test time was standardized to 60 s. If the filter

happened to clog before 60 s, the test time was shortened. The test period on the chart recorder was located knowing the starting time (time when the glass filter was inserted) and that a 90 s time delay is associated with the MTS output. This means that the output of the MTS for each test began 90 s after the insertion of the hood filter. The MTS was allowed to run 90 s after the filter was removed, and then was stopped. The protective channel was placed back in the stack until the next test.

Other data were also recorded during each test, including the CO and CO_2 concentrations in both the stack and dilution tunnel, thermocouple readings, and manometer reading. Also, the time between the beginning of the run (firing of the stove) and each test was recorded. Scale readings were recorded at four minute intervals throughout the run.

Two runs were made with 11 and 13 tests taken during the first and second runs respectively. During these runs, the primary air inlet was varied to cause different stack flow rates and burning rates. The tests throughout each run were taken at arbitrary times and the stove was reloaded as needed.

At the end of each run, the MTS was shut down by turning off the electrically operated equipment, emptying and drying the pressurized cylinder, and placing the protective channel in the stack. Sampling lines used in the sampling train were removed and cleaned and the blower was allowed to run for the duration of the stove burnout.

3.3 "Conventional" PAH Analysis

The samples collected by the hood filters were extracted with methylene chloride in a Soxhlet extractor for 24 hours. The solution within the flask was removed and evaporated to 1 ml. This sample was placed on the top of a column containing Silican Gel. Four solvents, 25 ml of hexane, 25 ml of 50% pentane in methylene chloride, 25 ml of methylene chloride, and 100 ml of 10% methanol in benzene were passed through the column. All the solvents were collected together and reduced to near dryness. Methylene chloride was then added to obtain the desired volume for the sample, typically 1 to 6 ml. One microliter of the sample was injected into an HP 5830 A gas chromatograph using a 5.5 metre SP 2100 column. A flame ionization detector was used.

A standard mixture of 16 compounds, Supelco, Inc. PAH mixture 610-M, and 2 individual compounds obtained from the U.S. Environmental Protection Agency were used to identify the PAH peaks on the gc curve. The actual compounds attempting to be quantified are give in Table I. These 18 compounds are representative of compounds used in other studies determining PAH emissions. Table I also shows the percentage of total PAH that these 18 compounds constitute in several other studies.

3.4 Collection Efficiency Test

Since the collection efficiency of the tape drawn through the stack is important to the performance of the MTS, a method was devised to test this phenomenon. The collection efficiency (e) is the ratio of particles impacted on the tape to the number that would have impacted if

TABLE I. PAH COMPOUNDS QUANTIFIED IN THIS STUDY COMPARED TO COMPOUNDS QUANTIFIED IN OTHER STUDIES.

Compounds Attempting to be Quantified in This Study

1. Naphthalene
2. Acenaphthene
3. Acenaphthylene
4. Fluorene
5. Phenanthrene
6. Anthracene
7. Fluoranthene
8. Pyrene
9. Benzo(a)anthracene
10. Chrysene
11. Benzo(b)fluoranthene
12. Benzo(k)fluoranthene
13. Benzo(a)pyrene
14. Indeno(1,2,3-c,d)pyrene
15. Dibenzo(a,h)anthracene
16. Benzo(g,h,i)perylene
17. 1 Methylnaphthalene
18. 2 Methylnaphthalene

Percentage of the Total PAH that the Above 18 Compounds Constitute in Other Studies

DeAngelis (6)	70%
Hangebrauck (8)	90%
Cooke (15)	93%
Hubble (17)	50-60%
Peters (18)	75%

the particles traveled in straight paths to the tape. This means that both parameters need to be determined simultaneously to calculate e. The apparatus in Fig. 8 was developed to accomplish this. The 6 mm diameter suction tube was placed through the center of the block of wood with one end flush to the bottom of the block. Air was drawn through the tube by a pump. A piece of filter paper tape the same width as the block was placed over the bottom of the block, completely covering it. The pump was turned on and the assembly was placed in the stack of the burning stove. The section of tape covering the suction tube had exhaust gases drawn through it and was used to represent the particles that would be collected at 100% efficiency. The rest of the tape was situated in the stack in the same manner as the MTS filter tape and was used to represent the particulate collection by the MTS. The device was left in the stack for 15 s, approximately the same time the MTS tape would be exposed to the flow. The flow through the suction tape was not accurately monitored during testing, but was known to be isokinetic or greater. This means that the particles collected beneath the tube represent 100% efficiency or more. Three tests were made at varied smoke densities.

The strips of tape were examined with a scanning electron microscope (SEM). Two 5 mm square sections, one from under the suction tube and one from between the end of the block and the suction tube were cut from each strip. The sections were mounted for examination by the SEM. A section of blank filter paper tape was also mounted for comparison.

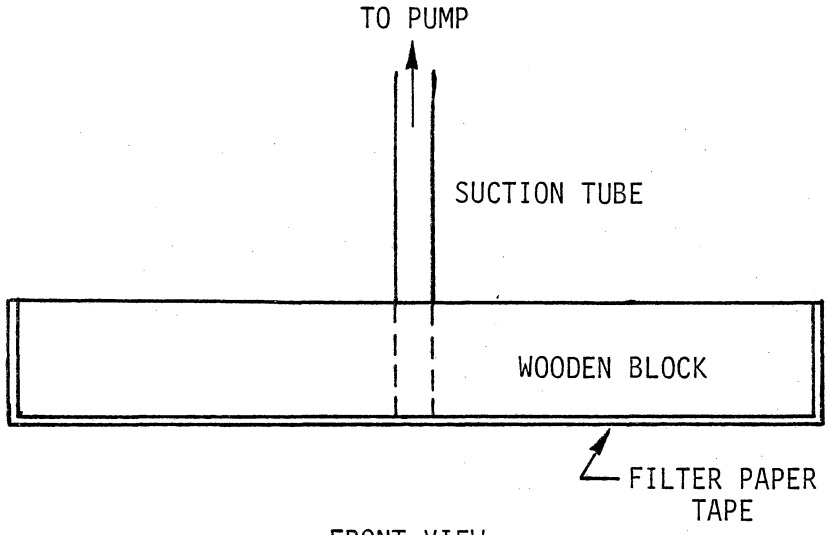

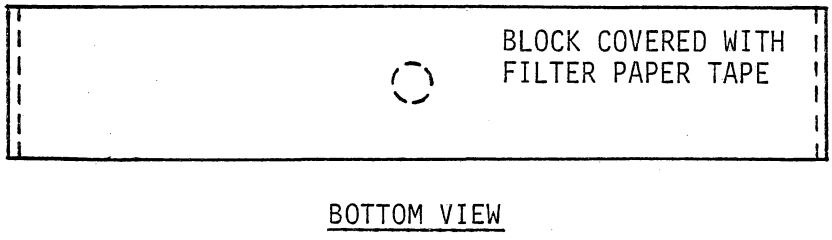

Figure 8. Apparatus Used for Testing the Collection Efficiency of the MTS

Each section was examined with the SEM and representative photos were taken of each.

4. RESULTS

4.1 Experimental Results

The results of runs 1 and 2 are shown in Tables II and III respectively. An explanation of how the results were obtained from the experimental data follows.

4.1.1 Flow Rates

The flow rate through the dilution tunnel was determined with the orifice plate in the tunnel. The flow rate in the stack was then found by equating the molar flow rates of CO_2 in the dilution tunnel and stack. A detailed description of this technique is given by Macumber and Jaasma (23).

4.1.2 Burning Rates

Plots of the scale readings taken for each run are given in Figs. 9 and 10 with the time of each test marked. The nominal burning rate of each test can be determined by the slope of the line in these plots. To verify this method, a conservative instantaneous burning rate was calculated from the molar flow rate of CO and CO_2 in the stack. Assuming that the major portion of carbon released during the combustion process leaves as CO and CO_2, an instantaneous burning rate can be calculated with the equation

$$\dot{m} = \frac{([CO]_s + [CO_2]_s)\ \dot{n}_s\ MW_C}{m_f} \qquad (1)$$

TABLE II. SUMMARY OF EXPERIMENTAL RESULTS FROM RUN 1. TEST CONDUCTED BURNING SEASONED OAK IN AN UPDRAFT MODE WITH THE SHENANDOAH (R-76LC) STOVE.

TEST	TEST TIME (s)	BURNING RATE (kg/hr)	STACK FLOW RATE (Nm^3/min)	MTS SIGNAL AREA (cm^2)	PAH EMISSIONS (mg)	PAH EMISSIONS (mg/kg)	CO EMISSIONS (%)	CO EMISSIONS (g/kg)
1	15	6.6	0.29	ND	4.0	150	3.5	110
2	75	2.4	0.18	6.3	2.6	52	2.5	130
3	105	1.8	0.13	0.4	0.03	0.6	1.9	93
4	60	4.5	0.28	2.0	0.04	0.4	0.9	36
5	60	4.2	0.16	3.0	0.02	0.3	0.5	30
6	60	3.9	0.51	1.5	0.002	0.1	0.6	50
7	60	3.6	0.31	8.8	0.002	0.1	1.8	100
8	60	3.6	0.33	8.1	0.02	0.3	2.1	130
9	60	3.9	0.22	6.9	3.1	48	2.1	83
10	60	1.8	0.18	2.3	4.0	140	2.1	140
11	60	1.8	0.18	1.5	0.2	5	2.3	150

ND - Not Done

TABLE III. SUMMARY OF EXPERIMENTAL RESULTS FROM RUN 2. TEST CONDUCTED BURNING SEASONED OAK IN AN UPDRAFT MODE WITH THE SHENANDOAH (R-76LC) STOVE.

TEST	TEST TIME (s)	BURNING RATE (kg/hr)	STACK FLOW RATE (Nm^3/min)	MTS SIGNAL AREA (cm^2)	PAH EMISSIONS (mg)	PAH EMISSIONS (mg/kg)	CO EMISSIONS (%)	CO EMISSIONS (g/kg)
12	30	4.2	0.33	2.1	0.06	1.7	1.7	90
13	45	4.8	0.28	13.6	0.63	10.	2.3	92
14	60	2.3	0.31	4.6	0.02	0.5	1.0	91
15	60	5.4	0.35	5.0	0.08	0.09	1.7	76
16	60	4.8	0.28	9.0	1.2	15.	1.6	65
17	60	3.3	0.26	2.5	0.55	10.	1.4	79
18	60	2.7	0.28	2.7	2.5	55.	1.5	65
19	60	3.9	0.50	0.0	NCD	NCD	0.2	15
20	60	3.1	0.49	0.0	0.000	0.0	0.2	18
21	60	2.4	0.43	0.0	0.001	0.0	0.3	30
22	30	4.8	0.41	ND	0.02	0.5	1.6	96
23	60	1.5	0.14	10.4	5.8	230.	2.7	190
24	60	1.2	0.11	10.0	4.1	210.	2.7	180

ND - Not Done
NCD - No Compounds Detected

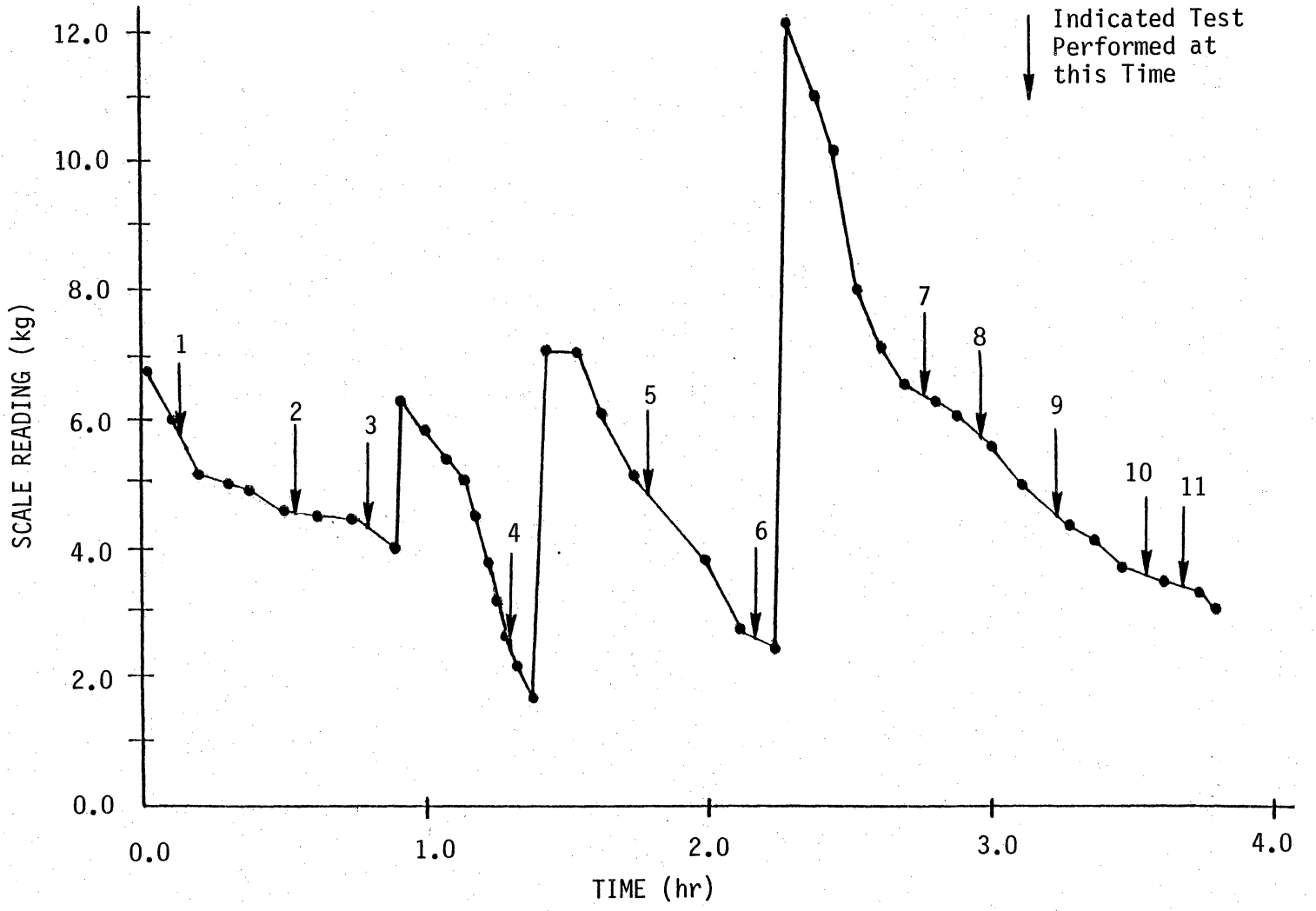

Figure 9. Mass-Time History Determined from the Scale Readings for each Charge Burned in Run 1.

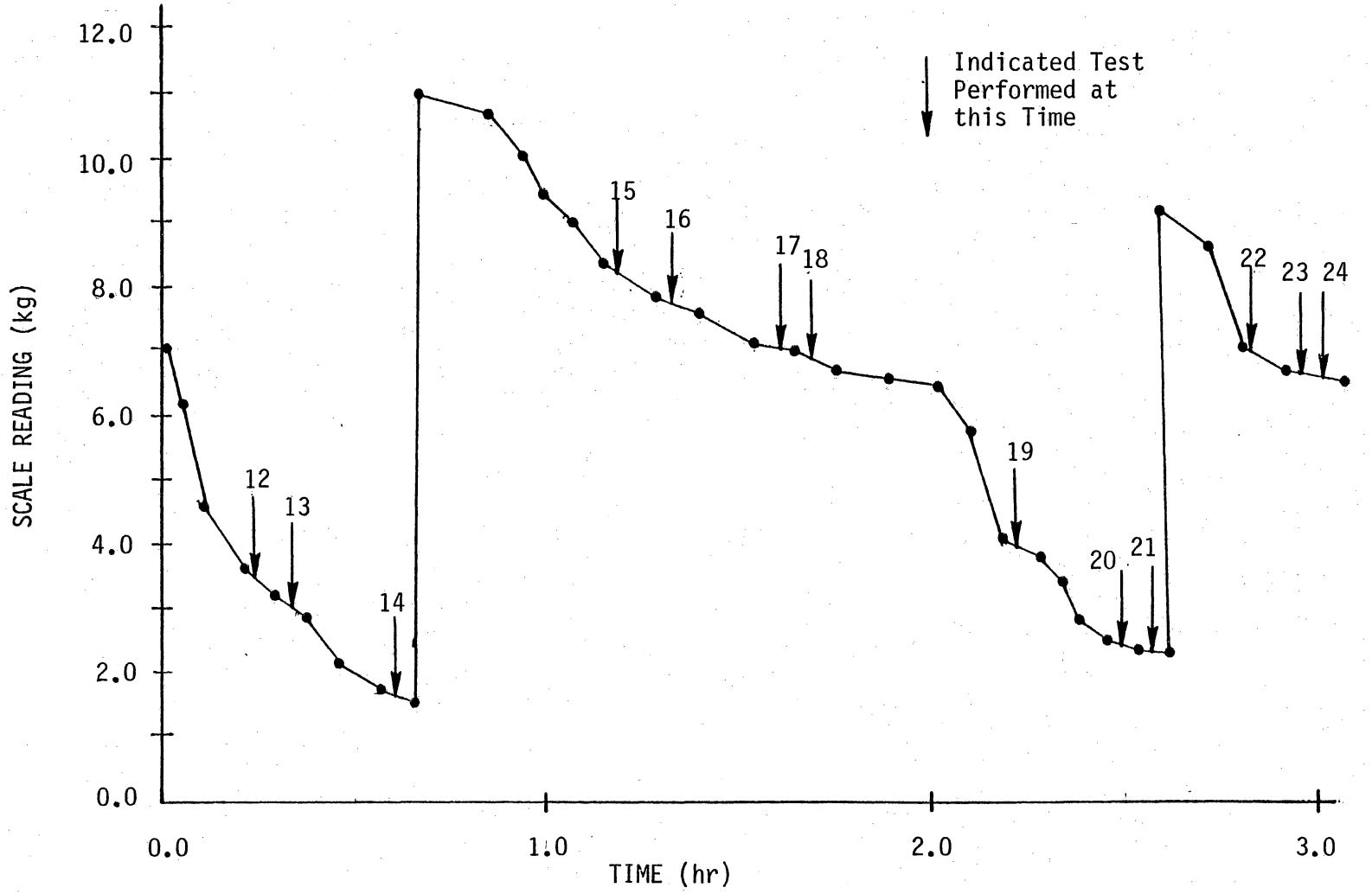

Figure 10. Mass-Time History Determined from the Scale Readings for each Charge Burned in Run 2.

where

$\dot{m}$ = the instantaneous burning rate, kg/s

$[CO_2]_s$ = mole fraction of CO_2 in the stack

$[CO]_s$ = mole fraction of the CO in the stack

$\dot{n}_s$ = molar gas flow rate in the stack, mol/s

MW_c = molecular weight of carbon, 12 g/mol

m_f = mass fraction of carbon in the wood assuming 10% moisture on a wet basis, 0.46 g carbon/g wet wood.

It is reported that CO and CO_2 can account for 90% of the carbon in a charge of wood (32), thus the burning rate of Eq. 1 should be a good approximation of the actual burning rate. The burning rate from the scale was usually slightly higher than that calculated by Eq. 1, except for a few tests which showed a higher instantaneous burning rate. In these cases the scale readings were assumed incorrect and the instantaneous value was used.

4.1.3 MTS Signal Area

An example of the MTS output is shown in Fig. 11. The zero line is obtained with the protective channel in the stack and shows the output of the photomultiplier tube as it responds to the fluorescence emitted by the sensitizer fluid only. This is taken as an indication of zero PAH. When tape with PAH-containing particulate matter reaches the photodetector, the MTS output increases as shown in Fig. 11. This signal is in some way representative of the amount of PAH on the tape.

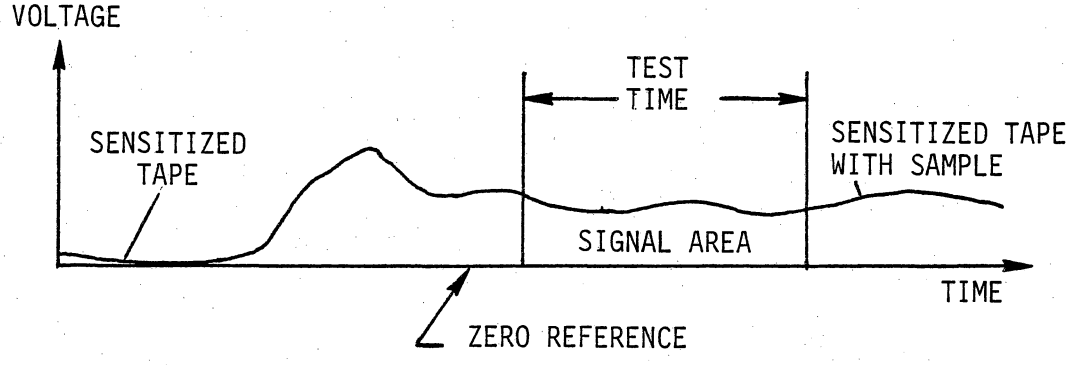

Figure 11. MTS Output from the Chart Recorder.

The MTS signal is integrated over the test time to obtain a signal area, which is taken to represent the total PAH collected on the tape during the test time. The integration is done by measuring the area under the curve and is shown as the MTS signal area in Tables II and III.

4.1.4 CO Emissions

The CO emissions are presented in Tables II and III as a dry percentage (read directly from the CO analyzer) and as an emission factor, which is given by

$$EF_{CO} = \frac{[CO]_s \ \dot{n}_s \ MW_{CO}}{\dot{m}} \qquad (2)$$

where

EF_{CO} = CO emission factor, g/kg

MW_{CO} = the molecular weight of CO, 28 g/mol,

4.1.5 PAH Emissions

The PAH emissions were determined from the gc analyses. The gc curve and the identified peaks for test number 15 are shown in Fig. 12. The total mass of PAH collected by each hood filter was determined by summing the individual masses of the compounds identified on the gc curve. The masses of the individual compounds detected in each test are given in Tables IV and V. To verify these results, the samples from the hood filters were analyzed twice or until two runs with results within at least 50% of each other were obtained. These two runs were averaged to get the mass of PAH which is presented in Tables II and III. The PAH

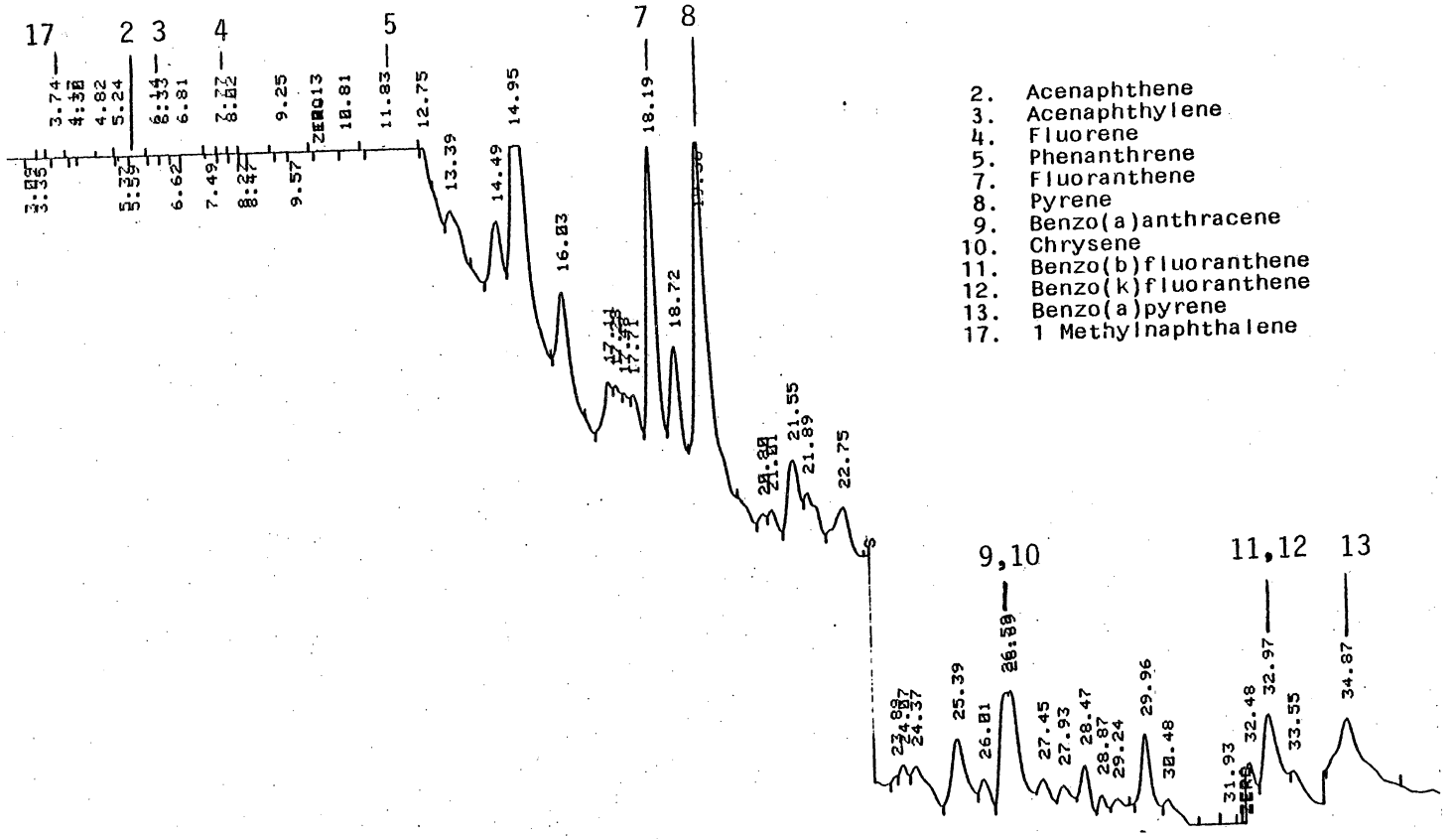

Figure 12. Gas Chromatography Curve with the Peaks Identified for Test 15.

TABLE IV. MASSES OF PAH COMPOUNDS (mg) IDENTIFIED IN RUN 1.

	TEST NUMBER										
	1	2	3	4	5	6	7	8	9	10	11
Naphthalene	ND	ND	ND	ND	ND	ND	ND	ND	ND	ND	ND
Acenaphthene	ND	ND	.005	.005	ND	ND	ND	ND	ND	ND	ND
Acenaphthylene	ND	.50	ND	ND	ND	ND	ND	ND	.032	.34	ND
Fluorene	ND	ND	.002	.012	ND	ND	ND	ND	ND	.006	ND
Phenanthrene	1.2	1.2	ND	ND	ND	ND	ND	.008	1.9	1.9	.005
Anthracene	.42	.28	ND	ND	ND	ND	ND	ND	ND	ND	ND
Fluoranthene	.54	.20	.001	.001	.003	ND	ND	.002	.10	.34	.018
Pyrene	1.0	.28	ND	.001	ND	.002	.002	.005	.56	1.2	.04
Benzo(a)anthracene/ Chrysene	.45	ND	.004	ND	ND	ND	ND	ND	ND	.12	.020
Benzo(b)fluoranthene/ Benzo(k)fluoranthene	.13	.03	.002	.017	ND	ND	ND	ND	.38	.13	.034
Benzo(a)pyrene	ND	ND	.012	ND	.016	ND	ND	ND	.14	ND	.038
Indeno(1,2,3-cd)pyrene	ND	ND	ND	ND	ND	ND	ND	ND	ND	ND	ND
Dibenzo(a,h)anthracene/ Benzo(g,h,i)perylene	ND	ND	ND	ND	ND	ND	ND	ND	ND	ND	ND
1 Methylnaphthalene	.30	.10	ND	ND	ND	ND	ND	ND	ND	ND	ND
2 Methylnaphthalene	ND	.05	.003	ND	ND	ND	ND	ND	ND	ND	ND
Total	4.0	2.6	.027	.036	.019	.002	.002	.015	3.1	4.0	.16

ND - Not Detected

TABLE V. MASSES OF PAH COMPOUNDS (mg) IDENTIFIED IN RUN 2.

	TEST NUMBER												
	12	13	14	15	16	17	18	19	20	21	22	23	24
Naphthalene	ND	ND	ND	ND	ND	ND	ND	ND	ND	ND	ND	ND	.39
Acenaphthene	.044	.008	ND	.003	.08	.15	ND	ND	ND	.005	.18	ND	ND
Acenaphthylene	ND	ND	ND	ND	ND	.008	.20	ND	ND	ND	ND	.26	.17
Fluorene	.016	.003	ND	ND	.048	ND	ND	ND	ND	ND	ND	.032	.032
Phenanthrene	.002	.003	ND	ND	.036	.24	1.2	ND	ND	.000	.009	2.3	1.9
Anthracene	ND	ND	ND	ND	ND	ND	ND	ND	ND	ND	ND	ND	ND
Fluoranthene	.002	.004	.005	.008	.06	.026	.36	ND	.000	.000	ND	.48	.50
Pyrene	ND	ND	.008	.009	.27	.20	.60	ND	ND	ND	.002	.76	1.0
Benzo(a)anthracene/ Chrysene	ND	ND	.000	.03	.084	ND	ND	ND	ND	ND	.002	.18	ND
Benzo(b)fluoranthene/ Benzo(k)fluoranthene	ND	ND	ND	ND	.16	ND	ND	ND	ND	ND	ND	.16	.13
Benzo(a)Pyrene	ND	.60	ND	.02	.56	ND	ND	ND	ND	ND	ND	.74	ND
Indeno(1,2,3-cd)Pyrene	ND	ND	ND	ND	ND	ND	ND	ND	ND	ND	ND	.46	ND
Dibenzo(a,h)anthracene/ Benzo(g,h,i)perylene	ND	ND	ND	ND	ND	ND	ND	ND	ND	ND	ND	ND	ND
1 Methylnaphthalene	ND	ND	ND	ND	ND	ND	ND	ND	ND	ND	ND	.28	ND
2 Methylnaphthalene	ND	ND	ND	ND	ND	ND	ND	ND	ND	ND	ND	ND	.000
Total	.064	.63	.018	.082	1.2	.55	2.5	.000	.000	.001	.018	5.8	4.1

ND - Not Detected

emission factors, also presented in Tables II and III, are given by

$$EF_{PAH} = \frac{M_{PAH}}{t \dot{m}} \qquad (3)$$

where

EF_{PAH} = PAH emission factor, g/kg

M_{PAH} = mass of PAH, g

t = test time, s.

4.2 Collection Efficiency Results

The results from examining the sections of filter tape with the SEM are presented in Figs. 13 - 16. Figure 13 shows tape that has not been placed in the gas stream. This "blank" shows tape that has not collected particles from the flue gas and is used to help identify particles collected in the test runs. The "blank" is magnified 1000 times. The results of two of the three tests for which SEM photos were taken are presented in Figs. 14 and 15, magnified 2000 times. Photos 14(a) and 15(a) are the sections of tape that had flow drawn through them by the suction tube, while photos 14(b) and 15(b) show the sections of tape that had no flow through them. The particles in photos (b) represent those that would be collected by the tape passing through the stack. Figure 16, a section of Fig. 14, is magnified 10,000 times and shows that the particles collected vary in size from 0.1 to 2.0 μm. The third test was taken during the end of a burn cycle (when particulate emissions are usually low), and consequently no particles were found on either section of tape and photos were not taken.

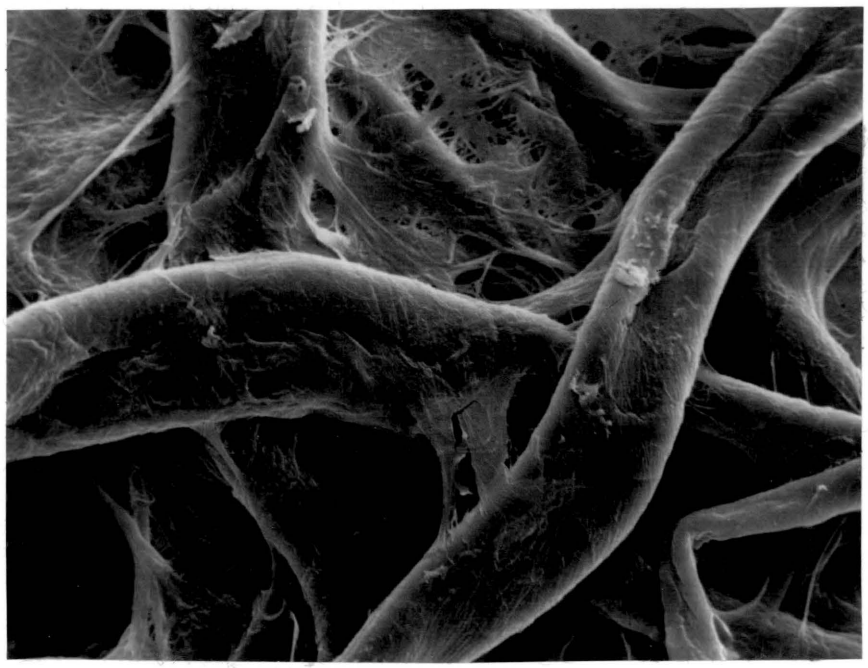

Figure 13. Appearance of "Blank" Filter Tape When Examined by the SEM (magnified 1000x).

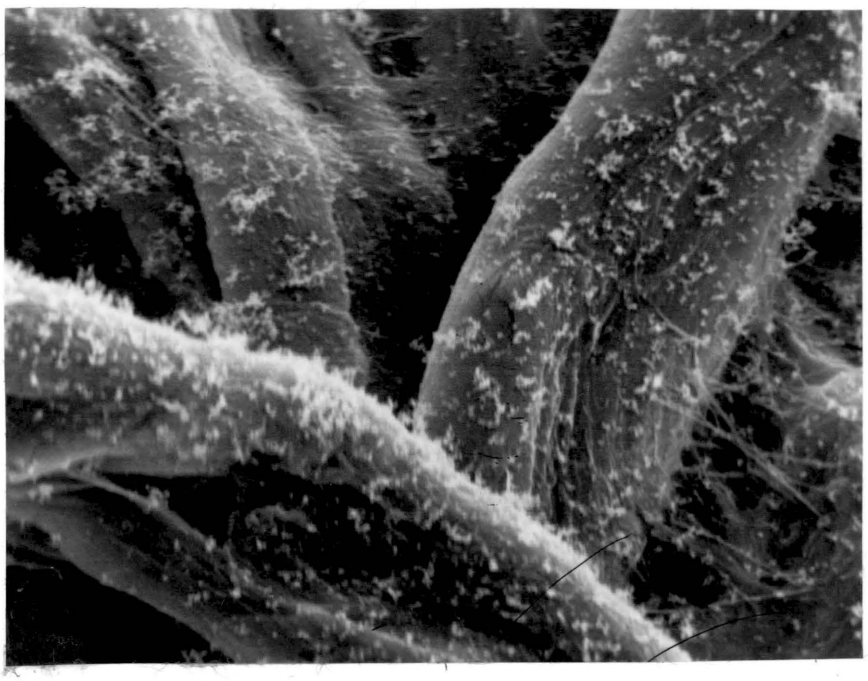

Figure 14(a). Appearance of Tape Representing 100% Collection Efficiency for Collection Efficiency Test 1 When Examined by the SEM (magnified 2000x).

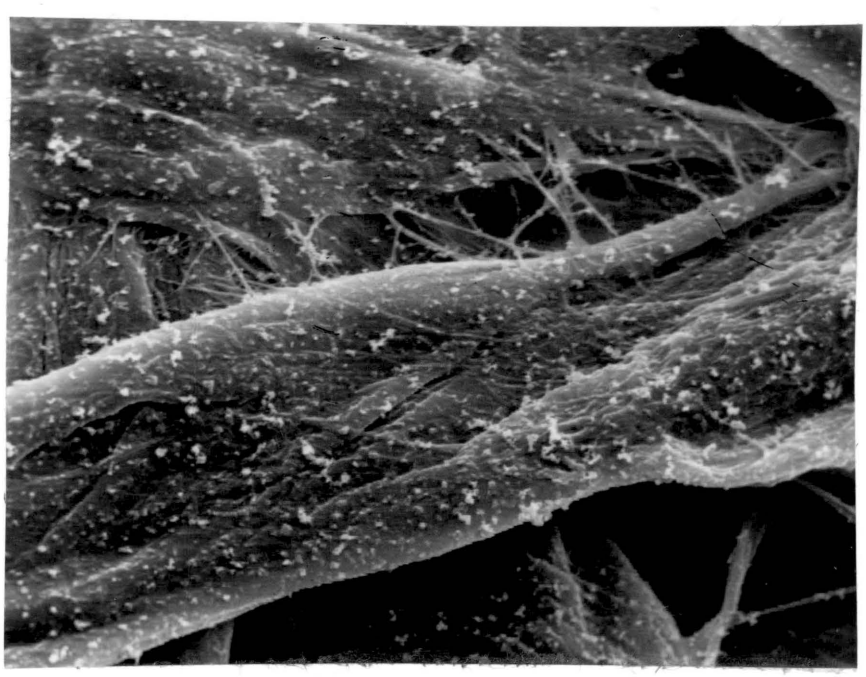

Figure 14(b). Appearance of Tape Representing MTS Collection for Collection Efficiency Test 1 When Examined by the SEM (magnified 2000x).

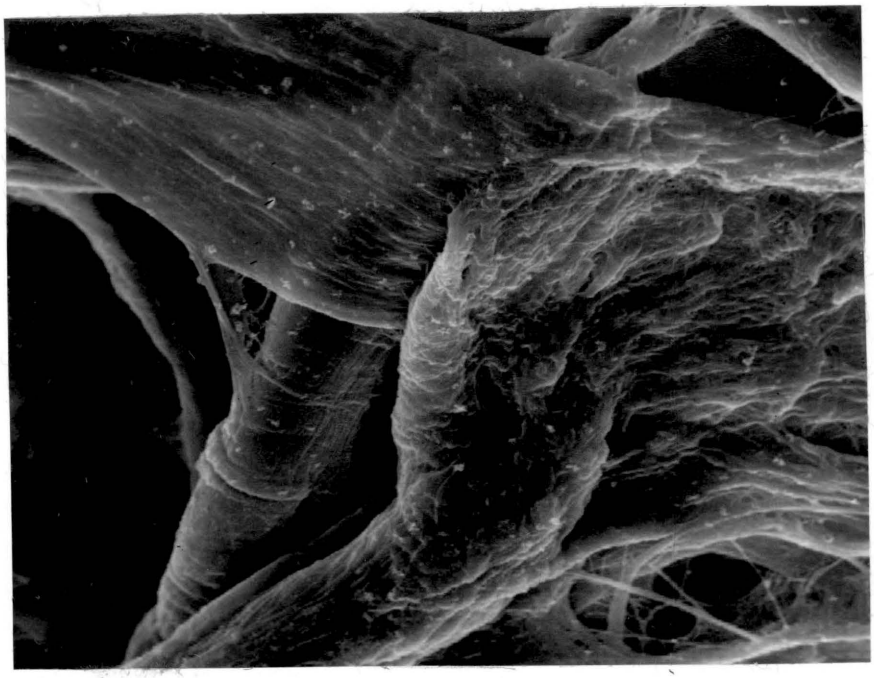

Figure 15(a). Appearance of Tape Representing 100% Collection Efficiency for Collection Efficiency Test 2 When Examined by the SEM (magnified 2000x).

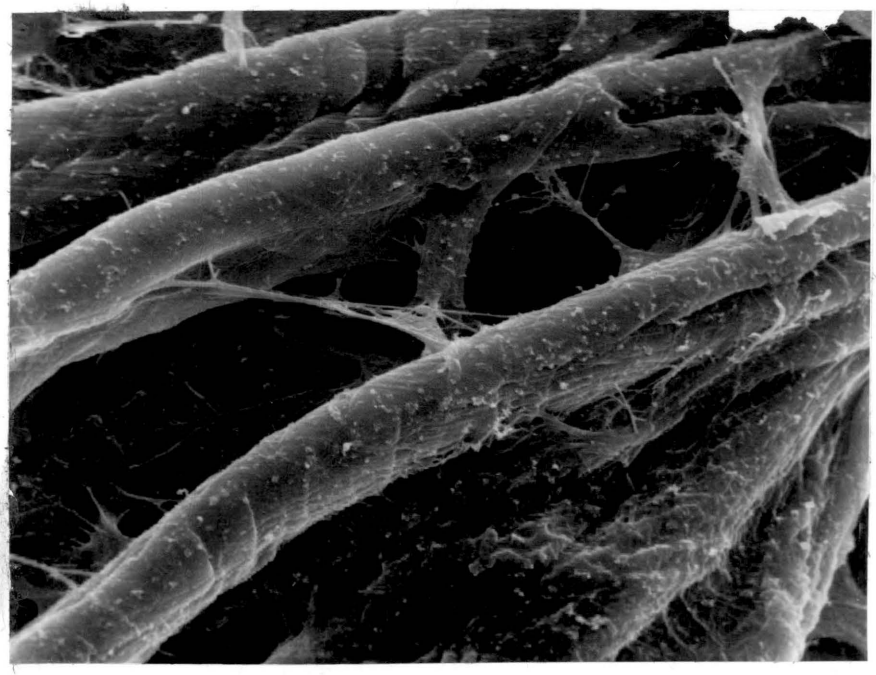

Figure 15(b). Appearance of Tape Representing MTS Collection for Collection Efficiency Test 2 When Examined by the SEM (magnified 2000x).

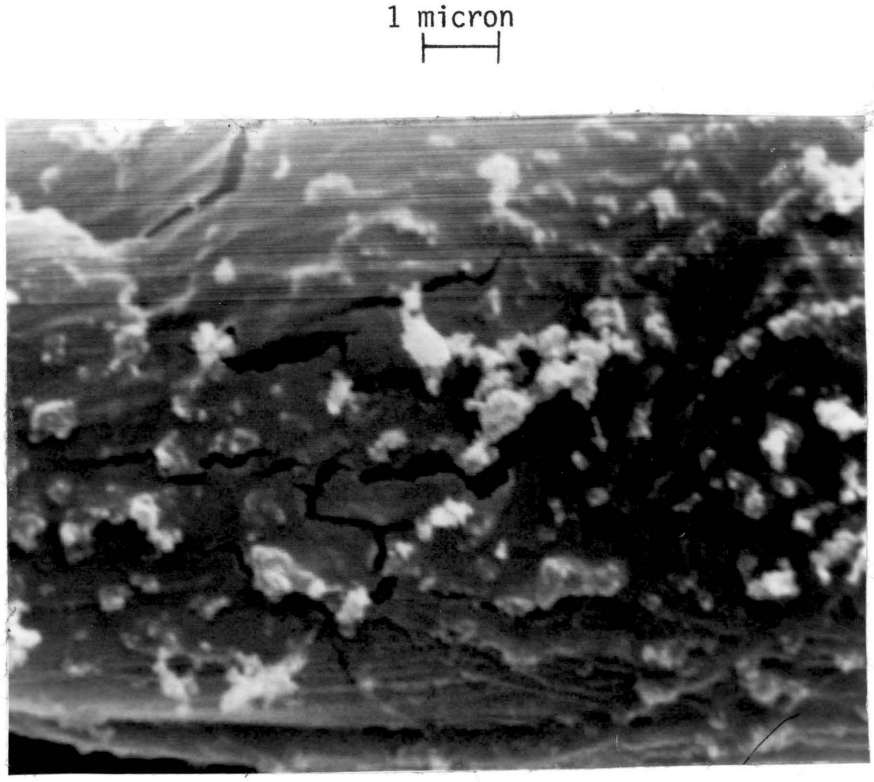

Figure 16. Particle Size Distribution Collected from the Smoke in Collection Efficiency Test 2 (magnified 10,000x).

5. DISCUSSION

5.1 Collection Efficiency

In an effort to estimate the collection efficiency of the MTS, inertial impaction is assumed to be the dominant mechanism of particle deposition on the tape. This assumption may be unjustified because of the particle size range being considered, which as shown by Fig. 16 is 0.1 to 2.0 μm. This range is the transition region between dominant deposition mechanisms, i.e. inertial impaction and diffusion. Assuming inertial impaction, the collection efficiency is calculated using the graph presented by Hawskley (30). In order to determine e (collection efficiency), the parameter K, defined as the ratio of the range of a particle to the width of the tape, must be determined. The collection efficiency is plotted against K, allowing the direct determination of e once K is found. To calculate K, a stack temperature of 150°C, a stack velocity of 0.7 m/s, and a particle Stokes' diameter of 1.0 μm (probably a high estimate) are assumed. The parameter K is calculated to be 1.0×10^{-3} as shown in Appendix 9.0. This value for K gives a negligible collection efficiency since a minimum K of 0.06 is needed before a value of e can be read from the graph.

The theoretical prediction of a negligible number of particles impinging on the tape from inertial impaction seems reasonable because of the low flow rates in the stack. Of course, as is seen in Figs. 14(b) and 15(b), particles are collecting on the tape while it is in the stack. One possible explanation for this is that collection by diffusion is the dominant mechanism. The particle deposition to the

tape by diffusion can be calculated but was not calculated in this study due to time limitations. A low stagnation pressure (1.0 Pa) at the lower surface of the tape eliminates flow through the tape as a possible explanation for particles collecting on the tape.

A comparison of photos (a) and (b) in Figs. 14 and 15 gives evidence of good collection efficiency by the tape in the stack. Although it is difficult to use the photos to assign a value to the collection efficiency, both Figs. 14 and 15 show that a significant number of the particles in the stack are being collected by the tape (assuming photos (a) represent 100% efficiency).

The relationship for the collection efficiency of the tape in the stack is not well understood because of the many factors that can affect the particle deposition rate to the tape. An involved analysis would be needed to develop a good theoretical model, and thus it appears that modifications to control the deposition rate are the better method of solving the problem. Such modifications are further discussed in Section 7.1.

5.2 MTS Performance

Although the relationship for the collection efficiency of the MTS is not understood, a correlation between PAH emissions and the MTS signal area is desired. Figure 17 is plotted in an attempt to see if such a relationship exists. It would be expected that an increase in PAH emissions would also cause an increase in the MTS signal area, but the data in Fig. 17 are too scattered to conclude any relationship.

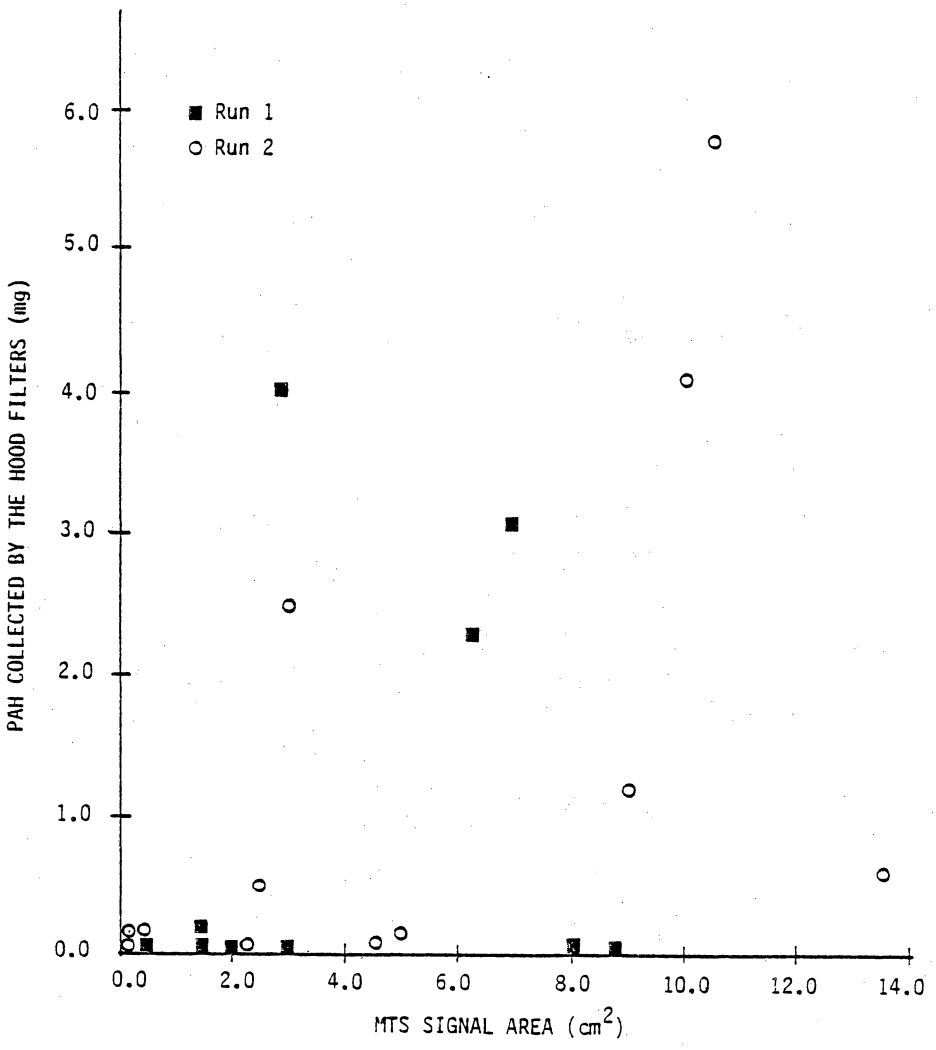

Figure 17. MTS Real-Time Results Compared to "Conventional" Results.

Several points, contradicting this expected relationship, show that the MTS gave a high signal while the PAH collected by the hood filter was nearly zero (less than 0.2 mg). Two other points seem to be an indication of low PAH (because of a low area), but instead have two of the highest amounts of PAH associated with them. These unexpected data points may be a result of problems with either the operation of the MTS or the analyses of the hood filters. Figure 17 does show good agreement between small signal areas and low PAH emissions, but some of these points may be a result of both poor compound identification and poor MTS performance.

The use of the hood filters for "conventional" PAH results to correlate the MTS results may not be an adequate method of comparison. The exhaust entering the collection hood is diluted with room air and thus is subject to a drop in temperature. The temperature difference between the thermocouple at the top of the stack and the thermocouple in the hood indicated a 40 to 50% drop in temperature (°C) from the stack gases to the hood mixture. The reduced temperature at the hood filter could increase condensation and cause more particulate matter to exist at the hood than at the MTS. The higher particulate count would most likely give more particulate PAH at the hood filter than at the MTS. Potentially, this situation might just cause a constant increase in the PAH results compared to the MTS signal and not really cause a problem in determining relative amounts of PAH. Conversely, this increase may not be constant with temperature, therefore adding a possible nonlinear effect on the relationship between the MTS signal and PAH results. This

situation is further complicated by the fact that the cooling due to dilution with room air is simultaneous with a reduction of the partial pressures of condensible species; it is not obvious whether condensation will increase or decrease.

Even if the MTS signal area was found to correlate well with the PAH results from the hood filters, the ability of the MTS to only detect particulate PAH may be a deficiency. Because gas-phase PAH traveling up the stack can not be detected by the MTS, it may underestimate PAH emissions. It appears that gas-phase PAH can sometimes account for 69 to 99% of the total PAH measured in the stack of a wood stove (15). Obviously, if only 1% of the PAH in the stack exists as particulate, the MTS would be useless. It is thought that the lower temperatures near the top of the stack (where the MTS samples) will cause higher percentages of particulate PAH. If a relationship between temperature and the percentage of gas-phase PAH could be determined, the MTS could possibly be used to determine total PAH. Further studies employing a method of measuring gas-phase PAH would be needed to verify this idea.

5.3 "Conventional" PAH Results

Table VI compares the PAH emission factors from this study with emission factors from other studies testing woodstoves. The average value from this study is in the middle of the other averages, but the range is the largest. The wider range of emission factors in this study compared to previous studies may be expected because of the different sampling times employed. The tests in this study are taken over a short

TABLE VI. SUMMARY OF PAH EMISSION FACTORS FROM STUDIES TESTING WOOD STOVES.

	EMISSION FACTOR RANGE (g/kg)	AVERAGE EMISSION FACTOR (g/kg)	NUMBER OF TESTS CONDUCTED
This Study	10^{-4}-0.23	0.038	24
DeAngelis (6)	0.19-0.32	0.27	4
Cooke (15)	0.01-0.05	0.032	5
Rudling (16)	0.005-0.14	0.043	5
Hubble (17)	0.004-0.008	0.006	2

interval of the burn cycle, and their results may vary because of fluctuations in PAH emissions during the cycle. The PAH results given in the literature are a result of testing over a significantly longer time period (up to several hours) and thus represent an average emission over the sampling period. With this technique, fluctuations that may occur in the PAH emissions are not detected.

Many of the PAH emission factors presented in Tables IV and V appear to be excessively low. The tables show that 13 tests indicated amounts of PAH collected less than 0.2 mg, which, using a typical burn rate of 3 kg/hr and a test time of 60 sec, gives an emission factor of 0.004 g/kg. Of the 30 literature values used in this study only 5 points are less than 0.004 g/kg and none of which are from wood stoves. It is possible that the many indications of low PAH emissions resulted because the tests were conducted during times of low PAH emissions in the burn cycle, but several tests with low PAH showed high MTS signal areas and high CO emissions. It is also seen in Tables IV and V that most of the low values can be attributed to only a few compounds being detected instead of low indications of many compounds. These points suggest a problem in the handling and analysis of the hood filters. All of the data must be looked at with an uncertainty of 50% just from the poor precision from the gc.

One possible source of error in this study may have resulted from degradation of the PAH compounds on the filters during storage. Lee, et al. (33) found that during storage the Gelman glass fiber filter had the second highest loss of PAH compounds of five types of filters tested.

The hood filters used in this study were left in storage for one to two days after testing, thus allowing for possible degradation of any PAH compounds collected. This apparently can only account for losses of 30 to 50%, and does not explain the many low indications of PAH emissions. Any future studies using glass fiber filters to collect samples should consider this problem.

Hubble, et al. (17) suggest that high burning rates will result in high PAH emissions. (They are the only ones in the literature to suggest this relationship.) To see if such a relationship exists for this study, PAH emission factors are plotted against burning rates in Fig. 18. The combined data from both runs show no definite relationship, although the data of run 2 alone tends to suggest that lower burning rates increase PAH emissions, just the opposite of Hubble's relationship. If any relationship were to exist in this study, the trend of the data from run 2 would seem likely since only particulate PAH is measured. It has been shown (34,35) that decreasing burn rates increase particulate emissions, which would seemingly increase PAH emissions in this study. Because of the conflicting ideas, a conclusion on the effect of burning rate on PAH emissions is not made.

5.4 PAH Emissions through a Burn Cycle

To look for patterns of PAH emissions throughout a burn cycle, Figs. 19 and 20 are plotted showing the PAH emission factors at the time of each test taken during runs 1 and 2 respectively. The MTS signal areas obtained during each test are also plotted. The times at which

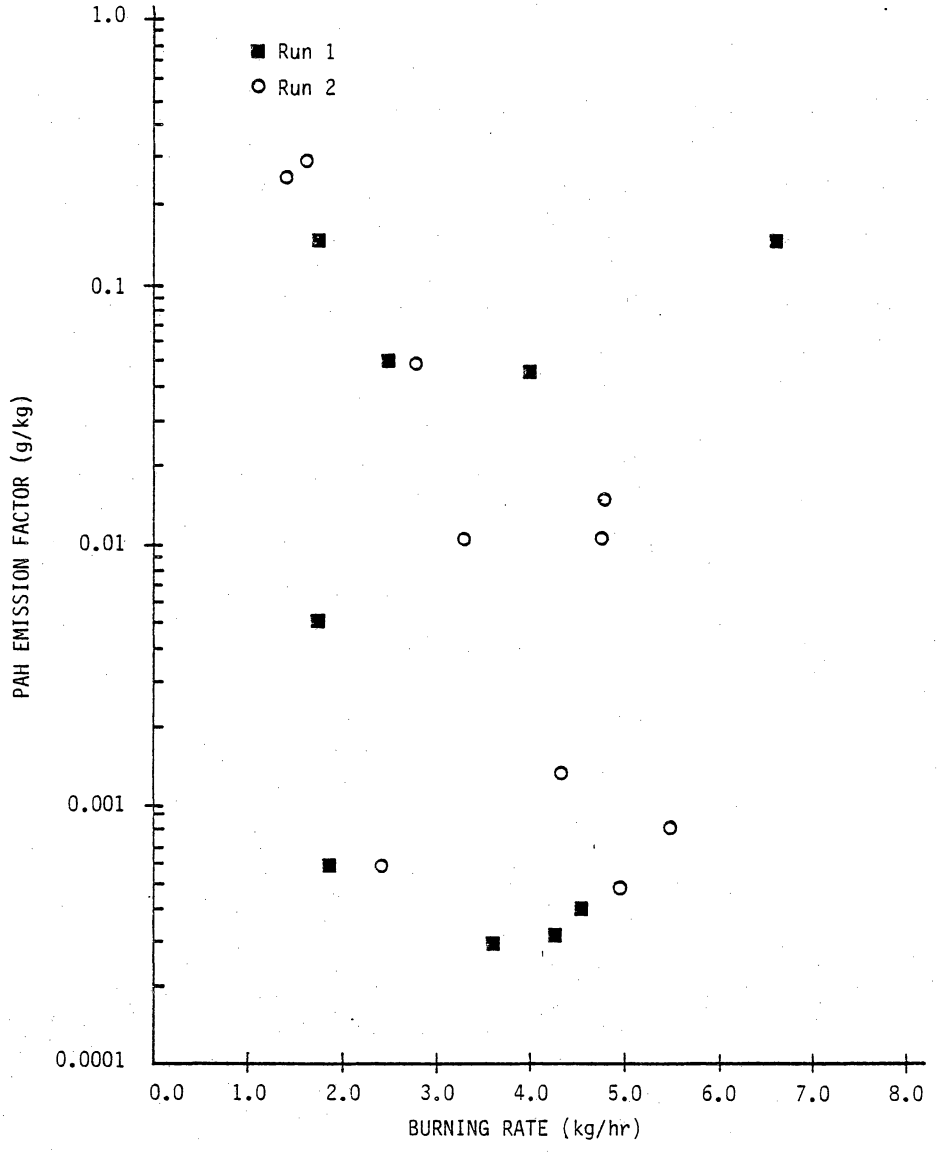

Figure 18. The Effect of Burning Rate on PAH Emissions.

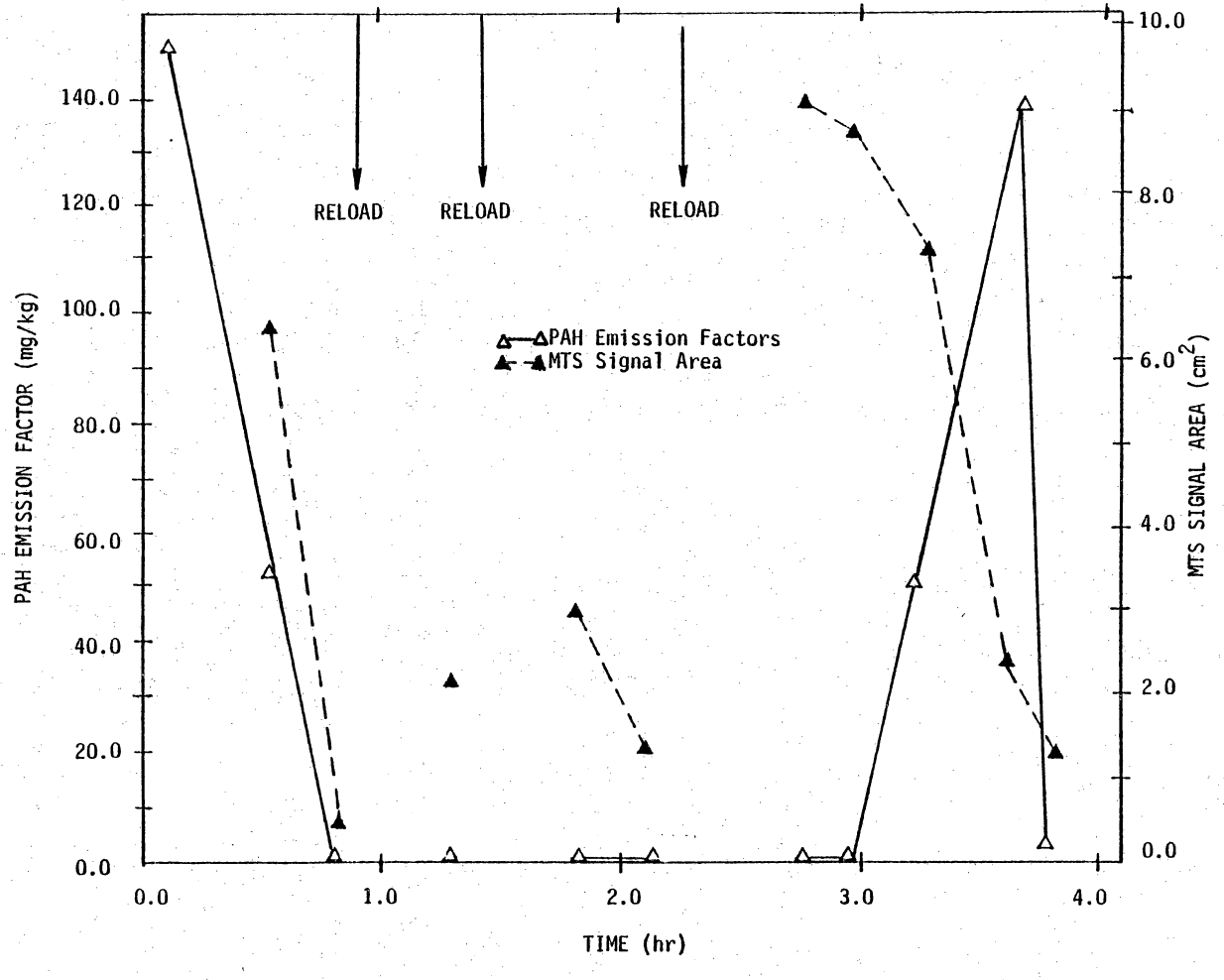

Figure 19. PAH Emissions throughout the Burn Cycles of Run 1

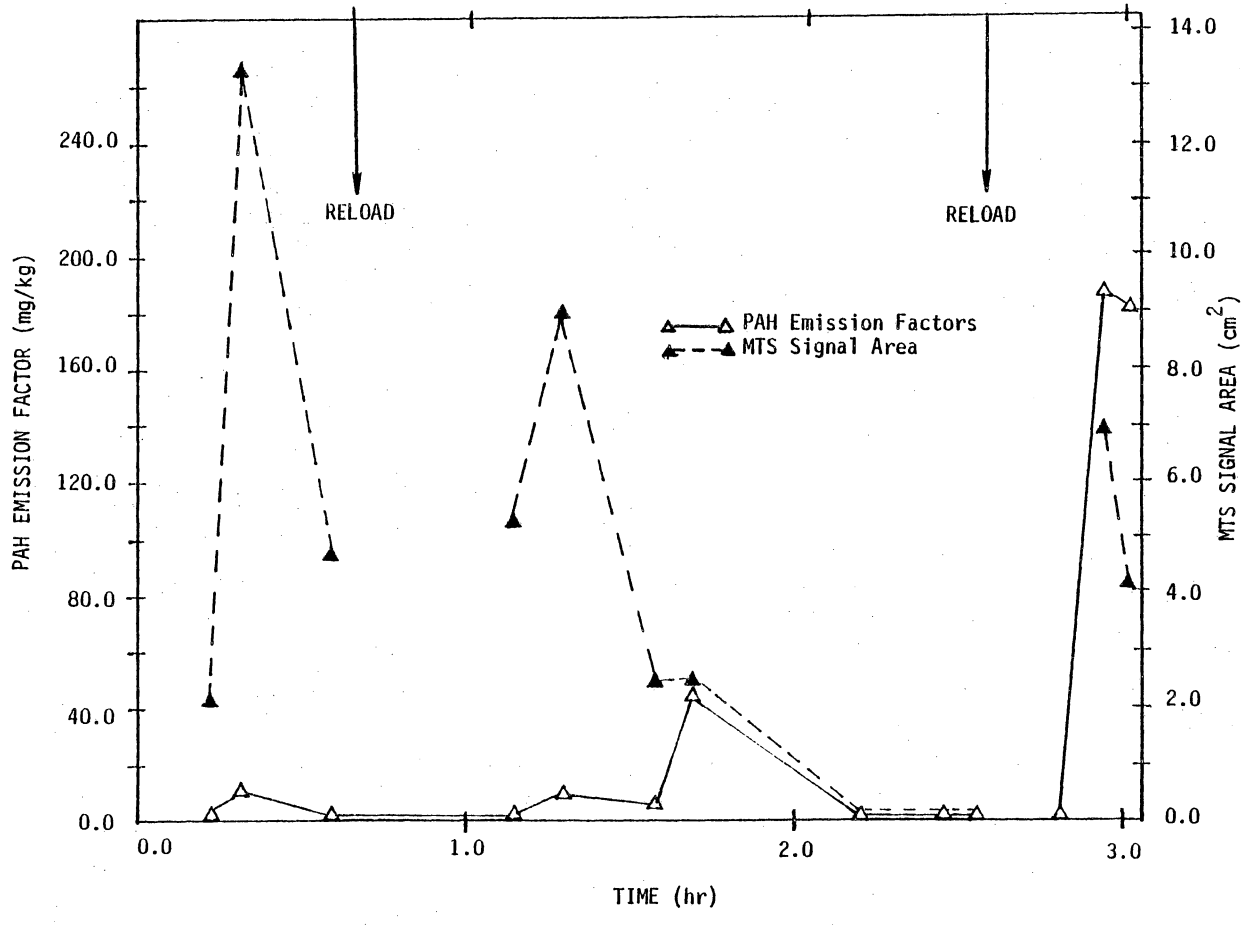

Figure 20. PAH Emissions throughout the Burn Cycles of Run 2.

the stove was reloaded are shown and indicate the beginning of a new burn cycle. It was thought that PAH emissions would be high in the beginning of the cycle and then gradually decline to a minimum value near the end of the cycle. This trend is only found in the first burn cycle of run 1 for the PAH emission factors. The MTS signal area agrees better with this idea since all cycles in run 1 (having more than 1 test) and one of the cycles in run 2 show a decline in signal area throughout the cycle. Because of the various trends in Figs. 19 and 20 a definite pattern for PAH emissions throughout a burn cycle is not evident.

5.5 Proxy Compounds

The data collected from the literature are presented graphically in Figs. 21 and 22. Figure 21 presents CO emission factors compared to PAH emission factors, while Fig. 22 gives the plot between NO_x and PAH emission factors. A log-log scale is used to plot the data because of the large variations in the emission factors. The use of proxies in this study is only being considered for residential wood and coal combustion, and thus the data in Figs. 21 and 22 are from these combustion systems only.

5.5.1 CO Emissions

Figure 21 also includes the data points from Tables II and III. Only the points greater than 0.001 g/kg are included, since some of the values below 0.001 g/kg are suspect. Two bands of data points showing

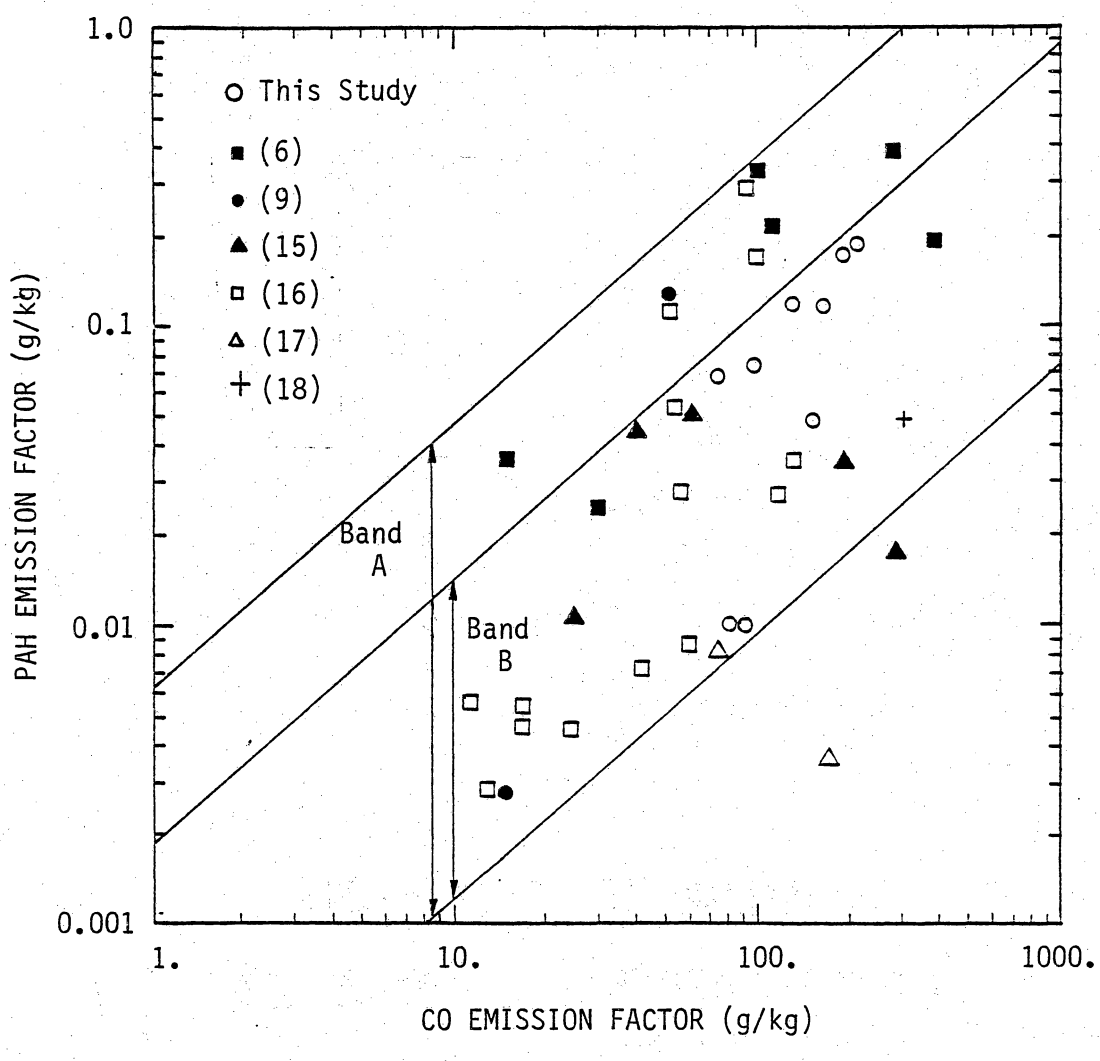

Figure 21. CO as a Possible Proxy for PAH Emissions from Residential Wood and Coal Combustion.

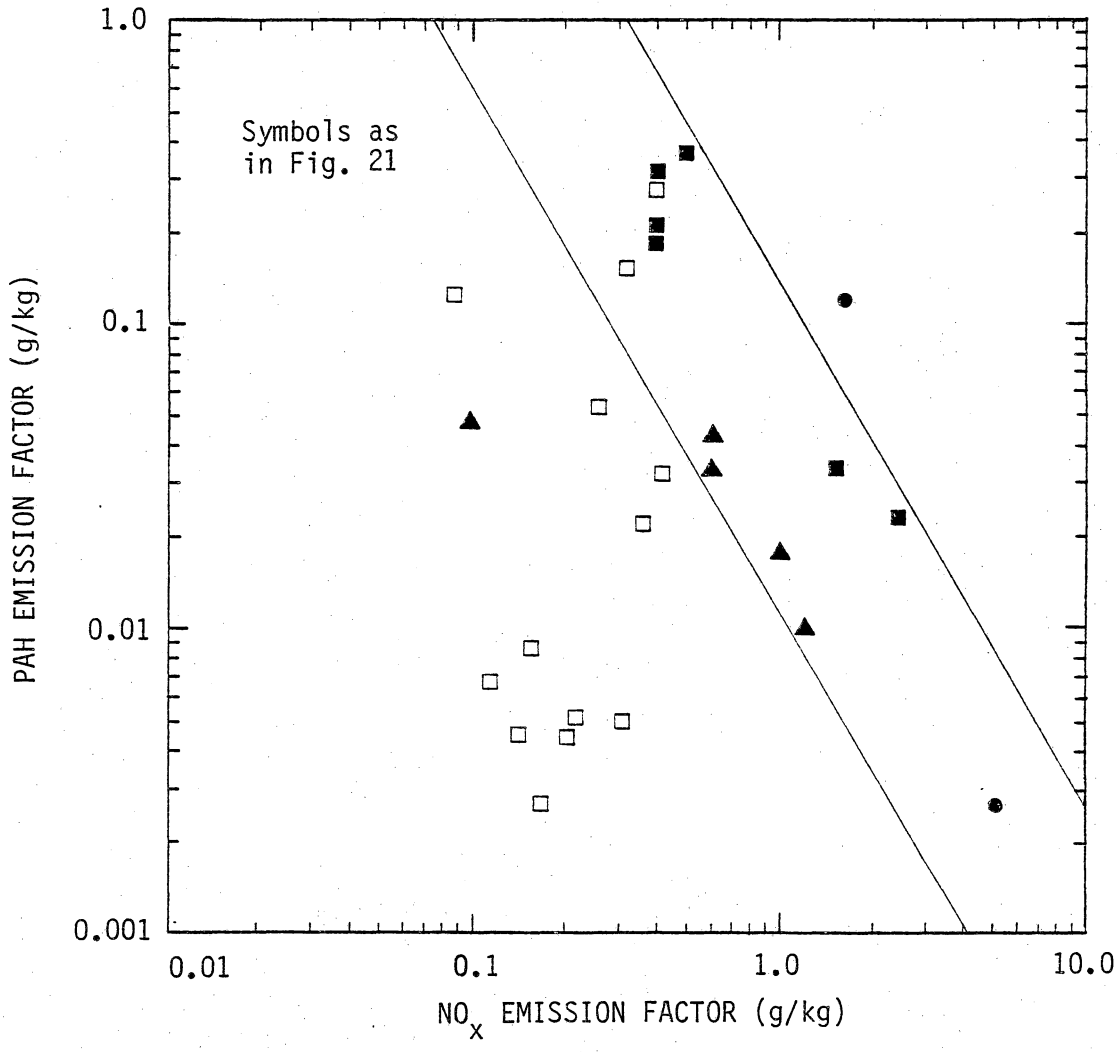

Figure 22. NO_x as a Possible "Inverse" Proxy for PAH Emissions from Residential Wood and Coal Combustion. (6, 9, 15, 16)

increasing PAH emissions factors with increasing CO emission factors have been made. Band A has a PAH emission factor range of one and a half orders of magnitude and includes all but four points. Band B leaves out several additional points, but only has a range of about one order of magnitude for the PAH emission factors. This size range is considered reasonable, since a standard method of measuring PAH emissions is not used for the various studies referenced. The data points from this study within band B show the same trend as the band but with a greater slope.

Although CO seems to be a reasonable proxy for PAH emissions, several possible conditions exist where it may not be valid. In the burn-out part of the burn cycle (where low PAH emissions would be expected), CO emissions have been reported to be high (31). Also, if Hubble is assumed correct, high burn rates may increase PAH emissions although it has been suggested that high burn rates decrease CO emissions (34,36). Both of these ideas tend to contradict Fig. 21 and CO should not be used as a proxy for PAH emissions during these situations. Testing at these conditions is not expected to be of major concern though, since high burning rates are not typically used in residential burning and the burn-out part of the burn cycle only accounts for a minor portion of a stove's use.

5.5.2 NO_x Emissions

The number of points in Fig. 22 is limited since NO_x emissions were not reported in all of the references included in Fig. 21. A band

showing an inverse relationship between NO_x emission factors is shown in Fig. 22. The band has a range of one order of magnitude for the PAH emission factors and suggests NO_x as an "inverse proxy" for PAH emissions. Unfortunately, the band only includes about half the data points, with most of the excluded points coming from the work of Rudling. Only two points from the others sources are not included in the band. The NO_x emission factors from Rudling are all in a small range (0.09 to 0.4 g/kg) and, considering that a variety of combustion systems were used in his study, a larger range would seem likely. Excluding the data from Rudling, NO_x emissions appear to have potential as an inverse proxy for PAH emissions.

The use of NO_x emissions as an inverse proxy may be difficult. The NO_x measurements reported in the different studies may be subject to uncertainties which are pointed out by Jaasma and Borman (37). They showed that NO can be bound to particulate matter and may not desorb for long periods of time. This reduces the measured NO_x emissions during testing, since only the gas-phase NO_x emissions are detected. Also, measured NO_x emissions may be too low, since some NO_2 (which is water soluble) is probably lost in the condensate of the condenser. Coals with high nitrogen contents may also present problems in using NO_x as an inverse proxy, since NO_x is then formed from N_2 in the air and fuel bound N. This could give unusually high NO_x emissions, which, if being used as an inverse indication of PAH emissions, would imply low PAH emissions.

Because of the limited reports of NO_x emissions in studies measuring PAH emissions and the uncertainties associated with these data, extreme caution should be exercised when considering NO_x emissions as an inverse proxy for PAH emissions.

6. CONCLUSIONS

This investigation has been hampered by the lack of a trusted "conventional" PAH measurement technique. Literature data for wood stove PAH emissions cover two orders of magnitude, and a significant amount of this variation is probably due to the use of different measurement techniques. The "conventional" technique employed in this study may be unreliable -- many tests yielded emissions factors that were an order of magnitude less than the lowest value reported in the literature (0.004 g/kg). Because of the uncertainties in the "conventional" results from the literature and this study, the real-time techniques investigated in this study have not been adequately evaluated. Therefore, the effectiveness of these techniques may be better (or worse) than the following conclusions. An adequate evaluation of the techniques can not be made until a standard "conventional" measurement technique is validated.

Of the three real-time techniques investigated, the use of CO as a proxy compound shows the most promise. Seventy one percent of the PAH emission factors from the literature and this study were included in a band having a range of one order of magnitude for the PAH emission factors. The use of CO as a proxy may be unreliable during the burn-out part of the burn cycle or during high burn rates, but PAH emissions in these modes of burning are not of great concern since they only account for a minor portion of a stove's use. The use of NO_x as an inverse proxy for PAH emissions shows some potential, but limited data and possible uncertainties associated with reported NO_x emission factors

leave doubt as to the reliability of NO_x as an inverse proxy. No definite relationship between the MTS and the "conventional" PAH results was found. If the "conventional" results are correct, the MTS did not work as expected.

The MTS has disadvantages in its present form. One is that its particulate collection efficiency is not known and may vary with stack conditions. Scanning electron microscope images confirm that particles of 0.1 to 2.0 μm did collect on the tape, but the dominant mechanism of this deposition is not know. The MTS can not measure gas-phase PAH and could give gross underestimations of PAH emissions, since large portions of the PAH in the stack could be in a gaseous form. This disadvantage might be overcome by using the MTS in the cooler environment of a dilution tunnel.

7. RECOMMENDATIONS

Based on the results of this study and other reports concerning PAH emissions, the author makes the following recommendations.

7.1 Real-Time PAH Measurement Techniques.

1) The MTS should be evaluated again once a reliable method for obtaining "conventional" PAH results is established.

2) The problem of not knowing the particulate deposition efficiency for the filter tape should be eliminated by modifications to the MTS. Methods of forcibly drawing exhaust gases through the tape should be explored.

3) More simultaneous NO_x and PAH emission factors should be obtained to test the usefulness of NO_x as an inverse proxy for PAH emissions from wood and coal stoves.

7.2 General PAH Measurements

4) A standard method of sampling and analyzing samples needs to be established. Included in this method should be a standard group of compounds used to compare PAH emissions from different studies. This standard group could be based on either carcinogenicity or typical stack concentrations. An accurate stack gas velocity measurement technique would also be an important part of this standard technique. A dilution tunnel (23) can be used for accurate velocity measurements.

5) A comparison of present techniques used to analyze PAH is needed to help determine how much of the emission factor range

in the literature is due to different analytical methods. A PAH sample in methylene chloride could be sent to selected groups for analysis, and the results could be compared.

6) Further studies investigating the effects of operating parameters and stove designs on PAH emissions should be conducted once a reliable measurement technique is validated.

8. REFERENCES

1. Sanborn, C. R., Poirot, R. L., Hoil, G. A., and M. A. Blanchet, "Waterbury Vermont: A Case Study of Residential Woodburning," Vermont Agency of Environmental Conservation, 2nd edition, August 1981.

2. Imhoff, R. E., Manning, J. A., Cooke, W. A., and T. L. Hayes, "Final Report on a Study of the Ambient Impact of Residential Wood Combustion in Petersville, Alabama," Proceedings of the Air Pollution Control Association Specialty Conference on Residential Wood and Coal Combustion, March 1-2, 1982, in press.

3. Peters, J. A., "POM Emissions from Residential Woodburning: An Environmental Assessment," in Residential Solid Fuels, (J. Cooper and D. Malek, eds.), Oregon Graduate Center, Beaverton, OR, 1982.

4. DeAngelis, D. G., Ruffin, D. S., and R. B. Reznick, "Source Assessment: Wood-Fired Residential Combustion Equipment Field Tests," U.S. Environmental Protection Agency Report No. EPA-600/2-79-019, 1980.

5. Smith, E. M., and P. L. Levins, "Sensitized Fluorescence Detection of PAH," in Chemical Analysis and Biological Fate: Polynuclear Aromatic Hydrocarbons (M. Cooke and A. Dennis, eds.), Battelle Press, Columbus, Ohio, 1980.

6. DeAngelis, D. G., Ruffin, D. S., and R. B. Reznik, "Preliminary Characterization of Emissions from Wood-Fired Residential Combustion Equipment," U.S. Environmental Protection Agency Report No. EPA-600/7-80-040, March 1980.

7. Butcher, S. S., and E. M. Sorenson, "A Study of Wood Stove Particulate Emissions," Journal of the Air Pollution Control Association, Vol. 29, No. 7, July 1979.

8. Gammage, R. B., and A. Bjorseth, "Proxy Methods and Compounds for Workplace Monitoring of Polynuclear Aromatic Hydrocarbons," in Polynuclear Aromatic Hydrocarbons: Chemistry and Biological Effects (A. Bjorseth and A. Dennis, eds.), Battelle Press, Columbus, Ohio, 1979.

9. Hangebrauck, R. P., Von Lehmden, D. J., and J. E. Meeker, "Emissions of Polynuclear Hydrocarbons and Other Pollutants from Heat Generation and Incineration Processes," Journal of the Air Pollution Control Association, Vol. 14, No. 7, 1964.

10. Sonnichsen, T. W., McElroy, M. W., and A. Bjorseth, "Use of PAH Tracers During Sampling of Coal Fired Boilers," in Polynuclear Aromatic Hydrocarbons: Chemistry and Biological Effects, loc. cit.

11. Diehl, E. K., Brevil, F. du, and R. A. Glenn, "Polynuclear Hydrocarbon Emissions from Coal Installations," Journal of Engineering for Power, April, 1967.

12. Particulate Polycyclic Organic Matter, National Academy of Sciences, Washington, D.C., 1972.

13. Giammer, R. D., Engdahl, R. B., and R. E. Barrett, "Emissions from Residential and Small Commercial Stoker-Coal-Fired Boilers Under Smokeless Operation," U.S. Environmental Protection Agency Report No. EPA 600/7-76-029, Oct. 1976.

14. DeAngelis, D. G., and R. B. Reznik, "Source Assessment: Coal-Fired Residential Combustion Equipment Field Tests," U.S. Environmental Protection Agency Report No. EPA 600/2-78-004, June 1977.

15. Cooke, W. M., Allen, J. M., and R. E. Hall, "Characterization of Emissions from Residential Wood Combustion Sources," in Residential Solid Fuels, loc. cit.

16. Rudling, L., Ahling, B., and G. Lofroth, "Chemical and Biological Characterization of Emissions from Combustion of Wood and Wood-chips in Small Furnaces and Stoves," in Residential Solid Fuels, loc. cit.

17. Hubble, B. R., Stetter, J. R., Gebert, E., Harkness, J. B. L., and R. D. Flotard, "Experimental Measurements of Emissions from Residential Wood Burning Stoves," in Residential Solid Fuels, loc. cit.

18. Peters, J. A., Hughes, T. W., and D. G. DeAngelis, "Wood Combustion Emissions at Elevated Altitudes," in Residential Solid Fuels, loc. cit.

19. Cooke, W. M., and J. M. Allen, "Trial Protcol for Sampling and Analysis of Emissions from Residential Wood Combustion," U.S. Environmental Protection Agency Report No. EPA 68-02-2686 task 131, 1981.

20. Pierce, T. L., and D. R. Jaasma, "Simplified Real-Time PAH Measurement Techniques," in Polynuclear Aromatic Hydrocarbons: Physical and Biological Chemistry, Battelle Press, Columbus, Ohio, 1982, in press.

21. Jaasma, D. R., and C. I. Metcalfe, "Real-Time Measurements of Emissions from an Airtight Woodstove," Paper No. CSS/CI-80-20, presented at the Spring Meeting of the Central States Section of the Combustion Institute, March 1980.

22. Wainwright, P. B., Aldridge, M. Y., Truesdale, R. S., and J. K. Ferrell, "A POM Emissions Study for Industrial Wood-Fired Boilers," North Carolina Department of Natural Resources and Community Development Division of Environmental Management," Raleigh, N.C., April, 1982.

23. Macumber, D. W., and D. R. Jaasma, "Efficiency and Emissions of a Hand-Fired Residential Coalstove," in Residential Solid Fuels, loc. cit.

24. Langmuir, I., "Mathematical Investigation of Water Droplet Trajectories," in The Collected Works of Irving Langmuir (C. Suits, ed.), vol. 10, Peragamon Press, N.Y., N. Y., 1977.

25. Johnstone, H. F., and M. H. Roberts, "Deposition of Aerosol Particles from Moving Gas Streams," Industrial and Engineering Chemistry, Vol. 41, No. 11, Nov. 1949.

26. Jordan, D. W., "The Adhesion of Dust Particles," in The Physics of Particle Size Analysis -- British Journal of Applied Physics, (supp. No. 3), The Institute of Physics, London, 1954.

27. Ungar, E. W., and A. A. Putnam, "The Physical Aspects of Deposition in Boiler and Gas-Turbine Systems," in A Review of Available Information on Corrosion and Deposits in Coal and Oil-Fired Boilers and Gas Turbines, American Society of Mechanical Engineers, 1959.

28. Golovin, M. N., and A. A. Putnam, "Inertial Impaction on Single Elements," Industrial and Engineering Chemistry Fundamentals, Vol. 1, No. 4, Nov. 1962.

29. Noll, K. E., and M. H. Pilat, "Inertial Impaction of Particles upon Rectangular Bodies," Journal of Colloid and Interface Science, Vol. 33, No. 2, June 1980.

30. Hawksley, P. G. W., Badzioch, S., and J. H. Blackett, Measurements of Solids in Flue Gases, 2nd edition, The Institute of Fuel, London, 1977.

31. Muhlbaier, J., "A Characterization of Emissions from Wood-burning Fireplaces," in Residential Solid Fuels, loc. cit.

32. Butcher, S. S., and M. J. Ellenbecker, "Particulate Emission Factors for Small Wood and Coal Stoves," in Residential Solid Fuels, loc. cit.

33. Lee, F. S. C., Pierson, W. R., and J. Ezike, "The Problem of Degradation During Filter Collection of Airborne Particulates -- An Evaluation of Several Commonly Used Filter Media," in Polynuclear Aromatic Hydrocarbons: Chemistry and Biological Effects, loc. cit.

34. Hubble, B. K., and J. B. C. Harkness, "Results of Laboratory Tests on Wood-Stove Emissions and Efficiency," Proceedings of Conference on Wood Combustion Environmental Assessment, Research Triangle Institute, Research Triangle Park, NC, 1981.

35. Kowalczyk, J. F., Bosserman, P. B., and B. J. Tombleson, "Particulate Emissions from New Low Emission Wood Stove Designs Measured by EPA Method 5," in Residential Solid Fuels, loc. cit.

36. Hayden, A. C. S., and R. W. Braaten, "Performance of Domestic Wood-Fired Appliances," Proceedings of Conference on Wood Combustion Environmental Assessment, Research Triangle Institute, Research Triangle Park, NC, 1981.

37. Jaasma, D. R., and G. L. Bowman, "Peculiarities Associated with the Measurement of Oxides of Nitrogen Produced by Diffusion Flames," Combustion Science and Technology, Vol. 23, No. 83, 1980.

9.0 APPENDIX

9.1 MTS Collection Efficiency Assuming Inertial Impaction as the Dominant Deposition Mechanism

The graph presented by Hawskley (30) is used to estimate the inertial impaction collection efficiency of the filter tape in the stack. The collection efficiency is plotted against a parameter K which is defined as

$$K = \lambda/L \tag{4}$$

where

λ = range of the particles being collected, m

L = width of the tape, m.

The range (λ) is given by

$$\lambda = vV/g \tag{5}$$

where

v = Stokes' velocity of the particles, m/s

V = stack gas velocity, m/s

g = local acceleration of gravity, 9.81 m/s^2.

The Stokes' velocity can be found from

$$v = (\sigma - \rho)\, g\, d^2/18\mu \tag{6}$$

where

σ = particle density, kg/m^3

ρ = density of stack gases, kg/m^3

μ = absolute viscosity of stack gases, Ns/m^2

d = Stokes' diameter of the particle, m

Substituting Eq. 6 into Eq. 5 yields

$$\lambda = \frac{V\ (\sigma - \rho)\ d^2}{18\mu} \tag{7}$$

The parameter K can be solved for by substituting Eq. 7 into Eq. 4, yielding

$$K = \frac{V\ (\sigma - \rho)\ d^2}{18\mu L} \tag{8}$$

Equation 8 can be further simplified to

$$K = \frac{V\ \sigma\ d^2}{18\mu L} \tag{9}$$

since $\sigma >> \rho$. To solve for K, typical values of V = 0.7 m/s, and μ = 2 x 10^5 Ns/m^2 (assuming a stack temperature of 150°C) are used for the stack gases while σ = 2000 kg/m^3 and d = 1 μm are assumed for the particles in the stack. The value of d = 1 μm is probably representative of the larger particles collected and will given an inflated collection efficiency. The width of the tape is known to be 2.54 cm, and thus K is found to be

$$K = \frac{(2000\ kg/m^3)(1 \times 10^{-6}\ m)(0.7\ m/s)^2}{(18)(2. \times 10^{-5}\ Ns/m^2)(0.0254\ m)}$$

$$K = 1.4 \times 10^{-4}$$

This value of K gives a value of zero for the collection efficiency from the graph, so the number of particles collected by inertial impaction must be negligible.

The vita has been removed from the scanned document

SIMPLIFIED REAL-TIME PAH MEASUREMENT TECHNIQUES

by

Timothy L. Pierce

(ABSTRACT)

The increased use of residential wood and coal stoves in recent years has caused a growing concern for polycyclic aromatic hydrocarbon (PAH) emissions from these stoves. Design of stoves that reduce PAH emissions has been hampered because existing PAH measurement techniques are slow, complex, and expensive. This study investigates two simple, inexpensive, real-time PAH measurement techniques which might be suitable for testing stoves. The first uses a device, called the "moving tape sampler" (MTS), that collects particulate samples on filter paper tape and uses sensitized flourescence to measure total PAH on the tape. The MTS results are compared to the results of a conventional PAH measurement technique, but no definite relationship between the two is found. Uncertainties about the conventional technique make it unclear whether one or both of the techniques give incorrect emission rates. The second method is the use of CO and NO_x as proxy compounds to infer PAH emissions. A plot of CO emission factors against PAH emission factors suggest CO as a proxy for PAH emissions while a similar plot for NO_x gives some evidence of NO_x being an "inverse" proxy for PAH emissions. The lack of a trusted PAH measurement technique has hampered the evaluation of both the MTS and proxy techniques.